

## Higgs triplets in the standard model

J. F. Gunion, R. Vega, and J. Wudka

*Department of Physics, University of California, Davis, California 95616*

(Received 6 April 1990)

Even though the standard model of the strong and electroweak interactions has proven enormously successful, it need not be the case that a single Higgs-doublet field is responsible for giving masses to the weakly interacting vector bosons and the fermions. In this paper we explore the phenomenology of a Higgs sector for the standard model which contains both doublet and triplet fields [under  $SU(2)_L$ ]. The resulting Higgs bosons have many exotic features and surprising experimental signatures. Since a critical task of future accelerators will be to either discover or establish the nonexistence of Higgs bosons with mass below the TeV scale, it will be important to keep in mind the alternative possibilities characteristic of this and other nonminimal Higgs sectors.

### I. INTRODUCTION

It is well known<sup>1</sup> that models with only Higgs  $SU(2) \times U(1)$  doublets (and, possibly, singlets) provide the most straightforward extensions of the standard model (SM) that satisfy constraints deriving from  $\rho \approx 1$  and the absence of flavor-changing neutral currents. However, there are many more complicated possibilities. For instance, conventional left-right-symmetric models are often constructed using a Higgs sector containing several triplet representations.<sup>2</sup> In those models, it is necessary to assign a very small vacuum expectation value to the neutral member of the left-handed triplet in order to avoid unacceptable corrections to the  $W$ - $Z$  mass ratio. However, it is certainly not necessary to go to left-right-symmetric extensions of the SM in order to consider Higgs-triplet fields. Even within the context of the SM a Higgs sector with Higgs-triplet as well as -doublet fields can be considered. Large tree-level deviations of the electroweak  $\rho$  parameter from unity can be avoided by two means: (i) the neutral triplet fields can be given vacuum expectation values that are much smaller than those for the neutral doublet fields; or (ii) the triplet fields and the vacuum expectation values of their neutral members can be arranged so that a custodial  $SU(2)$  symmetry is maintained. It is this latter type of model that we consider here. By custodial  $SU(2)$  at the tree level we mean simply that the hypercharges  $Y$  and vacuum expectation values  $V$  of all the Higgs multiplets are chosen so that  $\rho=1$  is maintained. More generally, one might hope that a model could be constructed that maintains a custodial  $SU(2)$  when loop corrections are included.

A number of models of type (ii), with a custodial  $SU(2)$  symmetry, have been proposed in the literature. In particular, we focus on the model constructed by Georgi and collaborators.<sup>3,4</sup> This model was considered in greater depth by Chanowitz and Golden,<sup>5</sup> who showed that a Higgs potential for the model could be constructed in such a way that it preserves the tree-level custodial  $SU(2)$  symmetry. This has the important implication that the custodial  $SU(2)$  is maintained after higher-order loop

corrections from Higgs self-interactions. Thus, the model provides an attractive example of an extension of the SM Higgs sector which contains Higgs triplets but no other new physics. We shall examine it with regard to the signatures and production mechanisms for the various Higgs bosons, focusing in particular on the singly and doubly charged Higgs bosons.

### II. BASIC FEATURES AND COUPLINGS OF THE HIGGS BOSONS

In the model of Ref. 3, the Higgs fields take the form

$$\phi = \begin{pmatrix} \phi^{0*} & \phi^+ \\ \phi^- & \phi^0 \end{pmatrix}, \quad \chi = \begin{pmatrix} \chi^0 & \xi^+ & \chi^{++} \\ \chi^- & \xi^0 & \chi^+ \\ \chi^{--} & \xi^- & \chi^{0*} \end{pmatrix}, \quad (2.1)$$

i.e., one  $Y=1$  complex doublet, one real ( $Y=0$ ) triplet, and one  $Y=2$  complex triplet. Following Ref. 3, we shall choose phase conventions for the fields such that  $\phi^- = -(\phi^+)^*$ ,  $\chi^{--} = (\chi^{++})^*$ ,  $\chi^- = -(\chi^+)^*$ ,  $\xi^- = -(\xi^+)^*$ , and  $\xi^0 = (\xi^0)^*$ . At the tree level, the masses of the gauge bosons are determined by the kinetic energy terms of the Higgs Lagrangian, which take the form

$$\mathcal{L}_{\text{kin}} = \frac{1}{2} \text{Tr}[(D_\mu \phi)^\dagger (D_\mu \phi)] + \frac{1}{2} \text{Tr}[(D_\mu \chi)^\dagger (D_\mu \chi)]. \quad (2.2)$$

Here,

$$D_\mu \phi \equiv \partial_\mu \phi + ig(\mathbf{W} \cdot \boldsymbol{\tau}/2)\phi - ig'\phi B \tau_3/2$$

and

$$D_\mu \chi \equiv \partial_\mu \chi + ig \mathbf{W} \cdot \mathbf{t} \chi - ig' \chi B t_3,$$

where the  $\tau_i/2$  are the usual  $2 \times 2$  representation matrices of  $SU(2)$  and the  $t_i$  are the  $3 \times 3$  representation matrices for  $SU(2)$  appropriate to the  $\chi$  representation we have chosen:

$$t_1 = \frac{1}{\sqrt{2}} \begin{pmatrix} 0 & 1 & 0 \\ 1 & 0 & 1 \\ 0 & 1 & 0 \end{pmatrix}, \quad t_2 = \frac{1}{\sqrt{2}} \begin{pmatrix} 0 & -i & 0 \\ i & 0 & -i \\ 0 & i & 0 \end{pmatrix}, \quad (2.3)$$

$$t_3 = \begin{pmatrix} 1 & 0 & 0 \\ 0 & 0 & 0 \\ 0 & 0 & -1 \end{pmatrix}.$$

It is useful to consider the transformation of the  $\phi$  and  $\chi$  fields under  $SU(2)_L \times SU(2)_R$ ,  $\phi \rightarrow U_L \phi U_R^\dagger$ , and  $\chi \rightarrow U_L \chi U_R^\dagger$ , where  $U_{L,R} = \exp(-i\theta_{L,R} \hat{n}_{L,R} \cdot \mathbf{T}_{L,R})$ , and the  $\mathbf{T}_{L,R}$  generators are represented as specified above. The  $SU(2)_L$  and  $U(1)$  invariances of the standard model are to be associated with  $\mathbf{T}_L$  and  $T_R^3$ , respectively. In particular, note that the  $U(1)$  hypercharge associated with the  $B$  field is represented by right multiplication by the appropriate  $T_R^3$  matrix (so that  $Q = T_L^3 + T_R^3$ ). The full  $SU(2)_R$  group will be associated with the custodial symmetry required to have  $\rho = 1$ . In particular, tree-level invariance for the gauge-boson-mass terms under the custodial  $SU(2)_R$  is arranged by giving the  $\chi^0$  and  $\xi^0$  the same vacuum expectation value. [However, since the hypercharge interaction with the  $B$  field breaks the custodial  $SU(2)_R$ , there are potentially infinite contributions to  $\rho - 1$  at one loop. We shall return to this issue later.] We define  $\langle \chi^0 \rangle = \langle \xi^0 \rangle = b$ , and also take  $\langle \phi^0 \rangle = a/\sqrt{2}$ . It will be convenient to use the notation

$$v^2 \equiv a^2 + 8b^2, \quad c_H \equiv \frac{a}{\sqrt{a^2 + 8b^2}}, \quad (2.4)$$

$$s_H \equiv \left[ \frac{8b^2}{a^2 + 8b^2} \right]^{1/2},$$

where  $c_H$  and  $s_H$  are the cosine and sine of a doublet-triplet mixing angle. We will also employ the subsidiary field

$$\phi^0 \equiv \sqrt{\frac{1}{2}}(\phi^{0r} + i\phi^{0i}), \quad \chi^0 \equiv \sqrt{\frac{1}{2}}(\chi^{0r} + i\chi^{0i}), \quad (2.5)$$

$$\psi^\pm \equiv \sqrt{\frac{1}{2}}(\chi^\pm + \xi^\pm), \quad \xi^\pm \equiv \sqrt{\frac{1}{2}}(\chi^\pm - \xi^\pm)$$

for the complex neutral and charged fields, respectively. The  $W^\pm$  and  $Z$  are given mass by absorbing the Goldstone bosons

$$G_3^\pm = c_H \phi^\pm + s_H \psi^\pm, \quad G_3^0 = i(-c_H \phi^{0i} + s_H \chi^{0i}). \quad (2.6)$$

The gauge-boson masses so obtained are

$$m_W^2 = m_Z^2 \cos^2 \theta_W = \frac{1}{4} g^2 v^2. \quad (2.7)$$

The remaining physical states can be classified according to their transformation properties under the custodial  $SU(2)$ . One finds a fiveplet  $H_5^{+,+,0,-,-}$ , a threeplet  $H_3^{+,0,-}$ , and two singlets,  $H_1^0$  and  $H_1^0$ . The compositions of the  $H$  states are

$$H_5^{++} = \chi^{++}, \quad H_5^+ = \xi^+, \quad H_3^+ = c_H \psi^+ - s_H \phi^+,$$

$$H_5^0 = \frac{1}{\sqrt{6}}(2\xi^0 - \sqrt{2}\chi^0), \quad H_3^0 = i(c_H \chi^{0i} + s_H \phi^{0i}), \quad (2.8)$$

$$H_1^0 = \phi^{0r},$$

$$H_1^{0r} = \frac{1}{\sqrt{3}}(\sqrt{2}\chi^{0r} + \xi^0).$$

[According to our phase conventions,  $H_5^{--} = (H_5^{++})^*$ ,  $H_5^- = -(H_5^+)^*$ ,  $H_3^- = -(H_3^+)^*$ , and  $H_3^0 = -(H_3^0)^*$ .] However, not all these states need be mass eigenstates. Only the doubly charged  $H_5^{+,+,-,-}$  and, for appropriately chosen phases, the  $H_3^0$  cannot mix. In general, the remaining neutral Higgs boson can mix with one another, as can the singly charged Higgs boson, depending upon the precise structure of the Higgs potential. The masses and compositions of the mass eigenstates are determined by the quartic interactions among the Higgs fields  $\phi$  and  $\chi$ . However, as we have already mentioned, it is desirable to choose the Higgs potential in such a way that it preserves the custodial  $SU(2)$  symmetry, as done in Ref. 5. In this case, the fiveplet and threeplet states cannot mix with one another or with the singlets; the only possible mixing is between  $H_1^0$  and  $H_1^{0r}$ . This latter mixing depends upon the parameters of the Higgs potential, and can range from zero to maximal. We shall adopt the language of zero mixing. Thus, we shall give results for couplings using the fields defined in Eq. (2.8).

From the Higgs-boson couplings to fermions and vector bosons we can determine the basic phenomenological features of the Higgs sector of the model. The fermion couplings have not been thoroughly studied in this model. There are two possible types. First, there are the standard Yukawa couplings of the doublet Higgs field to fermion-antifermion channels. We shall analyze these couplings in detail shortly. The only other possible couplings are ones closely analogous to those required in order to produce a "seesaw" mechanism for generating neutrino masses in left-right-symmetric models: namely, couplings of the triplet Higgs fields (with  $Y=2$ ) to the lepton-lepton channels. However, in the present context, where we envision expanding only the Higgs sector of the standard model, there are no right-handed partners for the neutrinos, and the introduction of such couplings leads directly to Majorana masses for the neutrinos. Limits on such Majorana masses for the neutrinos are quite restrictive, and will be reviewed shortly. In the case of the electron neutrino, they are sufficiently strong that even if the coupling in question assumes its upper-limit value, it will have no phenomenological impact.

The Lagrangian for Higgs-lepton-lepton interactions may be written in the form

$$\mathcal{L} = ih_{ij}(\psi_{iL}^T C \tau_2 \Delta \psi_{jL}) + \text{H.c.}, \quad (2.9)$$

where  $\psi_{iL}$  is the usual two-component leptonic doublet field,

$$\psi_{iL} = \begin{pmatrix} \nu_{iL} \\ l_{iL} \end{pmatrix}$$

$\Delta$  is a  $2 \times 2$  representation of the  $Y=2$  complex triplet field,

$$\Delta \equiv \begin{pmatrix} \frac{\chi^+}{\sqrt{2}} & -\chi^{++} \\ \chi^{0*} & -\frac{\chi^+}{\sqrt{2}} \end{pmatrix}, \quad (2.10)$$

and  $i, j$  are family indices. Expanding out this Yukawa interaction, we find Majorana mass terms for the neutrinos of the form

$$m_{ij} = 2h_{ij} \langle \chi^0 \rangle = \frac{h_{ij} s_H v}{\sqrt{2}}. \quad (2.11)$$

For simplicity, let us discuss the constraints on the  $h_{ij}$  assuming that this matrix is diagonal. The strongest limit on Majorana mass is that for  $\nu_e$  deriving from neutrinoless double- $\beta$  decay ( $\beta\beta_{0\nu}$ ). The experimental results imply<sup>6</sup> (with some uncertainty at the level of a factor of 2 due to nuclear questions) that  $m_{\nu_e} \lesssim 1$  eV. From this we use Eq. (2.11) to obtain  $h_{ee} \lesssim 5.75 \times 10^{-12}/s_H$ . For the muon and  $\tau$  neutrinos, the only useful limits are those obtained directly from  $\mu$  and  $\tau$  decays. For instance, in the case of  $\nu_\tau$  we have  $m_{\nu_\tau} \lesssim 35$  MeV,<sup>7</sup> implying  $h_{\tau\tau} \lesssim 2 \times 10^{-4}/s_H$ . Whether or not couplings that saturate these limits can be phenomenologically relevant is determined by the extent to which lepton-lepton channels can be of significance in the decays of the Higgs bosons. (The limits above clearly imply that the couplings are not useful for Higgs-boson production.) A typical example, to which we shall return later, is the decay  $H_5^{++} \rightarrow l^+ l^+$ . The relevant Feynman rule coupling for this decay is easily obtained from Eq. (2.9), and takes the form  $2h_{ll} v^T(k) C P_L v(l)$ , where  $P_L = (1 - \gamma_5)/2$ ,  $C$  is the usual charge-conjugation matrix, and  $k$  and  $l$  are the momenta of the two positively charged leptons. The resulting decay width is

$$\Gamma(H_5^{++} \rightarrow l^+ l^+) = \frac{|h_{ll}|^2}{8\pi} m_{H_5}. \quad (2.12)$$

We shall use these results in a later section to argue that these decays are rather unlikely to be phenomenologically important unless  $s_H$  is very small.

Returning to the standard doublet fermion-antifermion interactions, we see that all tree-level Higgs-boson couplings to fermion-antifermion channels are determined by the overlap of the mass-eigenstate Higgs fields with the doublet field. One finds that the  $H_5^{+,+,-}$ ,  $H_5^{+,-}$ ,  $H_5^0$ , and  $H_1^0$  states have no such overlap, and that only the  $H_3^{+,-}$ ,  $H_3^0$ , and  $H_1^0$  will have tree-level fermion-antifermion couplings. The Feynman rules for the various couplings are given below (to be multiplied by an overall factor  $i$ ):

$$\begin{aligned} g_{H_1^0 q\bar{q}} &= -\frac{gm_q}{2m_W c_H} \quad (q = t, b), \\ g_{H_3^0 t\bar{t}} &= +\frac{gm_t s_H}{2m_W c_H} \gamma_5, \\ g_{H_3^0 b\bar{b}} &= -\frac{gm_b s_H}{2m_W c_H} \gamma_5, \\ g_{H_3^- i\bar{b}} &= \frac{g s_H}{2\sqrt{2} m_W c_H} [m_t(1 + \gamma_5) - m_b(1 - \gamma_5)], \end{aligned} \quad (2.13)$$

where third-generation notation is employed for the quarks. Analogous expressions hold for the couplings to

leptons. As pointed out in Ref. 5 it is possible that  $b \gtrsim a$ , so that most of the mass of the  $W$  and  $Z$  comes from the triplet vacuum expectation values. In this case, the doublet vacuum expectation value  $a/\sqrt{2}$  is much smaller than in the SM, and the Yukawa couplings of the doublet to the fermions must be much larger than in the SM in order to obtain the experimentally determined quark masses. Then, the Higgs bosons that do couple to fermions have much larger fermion-antifermion pair couplings and decay widths than in the SM.

Most interesting, however, are the couplings to vector bosons. The Feynman rules for these are specified for the states of Eq. (2.8) as follows (we drop an overall factor of  $ig_{\mu\nu}$ ):

$$\begin{aligned} H_5^{++} W^- W^-: & \sqrt{2} g m_W^3 s_H, \\ H_5^{+} W^- Z: & -g m_W s_H / c_W, \\ H_5^{+} W^- \gamma: & 0, \\ H_3^0 W^- W^+: & (1/\sqrt{3}) g m_W s_H, \\ H_3^0 Z Z: & -(2/\sqrt{3}) g m_W s_H c_W^{-2}, \\ H_1^0 W^- W^+: & g m_W c_H, \\ H_1^0 Z Z: & g m_W c_H c_W^{-2}, \\ H_1^0 W^- W^+: & (2\sqrt{2}/\sqrt{3}) g m_W s_H, \\ H_1^0 Z Z: & (2\sqrt{2}/\sqrt{3}) g m_W s_H c_W^{-2}, \end{aligned} \quad (2.14)$$

where  $s_W$  and  $c_W$  are the sine and cosine of the standard electroweak angle, respectively. Several features of these couplings should be noted. First, there are no couplings of the  $H_3$  Higgs-multiplet members to vector bosons. Second, we observe that the SM is regained in the limit where  $s_H \rightarrow 0$ , in which case the  $H_1^0$  plays the role of the SM Higgs boson and has SM couplings, not only to  $VV$  channels as seen in Eq. (2.14), but also to  $f\bar{f}$  channels, Eq. (2.13). However, in this model with custodial SU(2) symmetry, there is no intrinsic need for  $s_H$  to be small. A third important observation is that when  $s_H \neq 0$  there is a nonzero  $H_5^{+} W^- Z$  coupling, in contrast with the absence of such a coupling of the charged Higgs boson in any model containing only Higgs doublets (and singlets).<sup>1</sup> In fact, one can demonstrate that any model containing triplet or higher Higgs bosons representations with a neutral field member that has a nonzero vacuum expectation value, and that simultaneously yields  $\rho = 1$  at the tree level, must have at least one charged Higgs boson with nonzero coupling to the  $WZ$  channel. Finally, we emphasize the remarkable dichotomy between the  $H_5$  and the  $H_3$  multiplets: Ignoring for the moment the  $HV$ - and  $HH$ -type channels, at the tree level the former couple and decay only to vector-boson pairs, while the latter couple and decay only to fermion-antifermion pairs.

However, to be complete, we must consider the couplings of the Higgs bosons to a vector boson and another Higgs boson, or to two other Higgs bosons. The latter couplings are model dependent and will be considered shortly. First, we give the Feynman rules for the former couplings. They are specified below in the convention

where we remove an overall factor of  $ig(p-p')^\mu/2$  for the  $W$  couplings, a factor of  $ig(p-p')^\mu/(2c_W)$  for the  $Z$  couplings, and a factor of  $ie(p-p')^\mu$  for the  $\gamma$  couplings [with  $p$  ( $p'$ ) being the incoming momentum of the Higgs boson listed first (second)]:

$$\begin{aligned}
H_1^0 H_3^- W^+ &: -s_H, \\
H_1^0 H_5^- W^+ &: 0, \\
H_1^{0'} H_3^- W^+ &: \frac{2\sqrt{2}}{\sqrt{3}} c_H, \\
H_1^{0'} H_5^- W^+ &: 0, \\
H_3^0 H_3^- W^+ &: \frac{1}{\sqrt{3}} c_H, \\
H_3^0 H_5^- W^+ &: -\sqrt{3}, \\
H_3^0 H_5^- W^+ &: -c_H, \\
H_3^0 H_3^- W^+ &: -1, \\
H_5^+ H_5^- W^+ &: -\sqrt{2}, \\
H_3^+ H_5^- W^+ &: -\sqrt{2} c_H, \\
H_3^0 H_1^0 Z &: s_H, \\
H_3^0 H_1^{0'} Z &: -\frac{2\sqrt{2}}{\sqrt{3}} c_H, \\
H_3^0 H_3^0 Z &: \frac{2}{\sqrt{3}} c_H, \\
H_5^- H_3^+ Z &: c_H, \\
H_3^- H_3^+ Z &: 2s_W^2 - 1, \\
H_5^- H_5^+ Z &: 2s_W^2 - 1, \\
H_5^- H_5^+ Z &: 2 - 4s_W^2, \\
H_3^- H_3^+ \gamma &: -1, \\
H_5^- H_5^+ \gamma &: -1, \\
H_5^- H_5^+ \gamma &: 2.
\end{aligned} \tag{2.15}$$

We note that, in our convention, the  $f\bar{f}Z$  and  $f\bar{f}\gamma$  couplings are given by

$$\begin{aligned}
f\bar{f}Z &: -i(g/c_W)\gamma^\mu [P_L(T_3 - Q \sin^2\theta_W) \\
&\quad + P_R(-Q \sin^2\theta_W)], \\
f\bar{f}\gamma &: -ieQ.
\end{aligned} \tag{2.16}$$

Here  $T_3 = \pm\frac{1}{2}$  and  $Q$  are the weak isospin and charge (in units of  $e$ ) of the fermion, e.g.,  $T_3 = -\frac{1}{2}$  and  $Q = -1$  for the electron. Some care is required in charge conjugating the  $W$  couplings listed in Eq. (2.15) because of the phases

and conjugation properties of the fields we employ. Following the same conventions given prior to Eq. (2.15), the rule is easily stated: The charge-conjugate coupling table is obtained by changing the signs of all entries (keeping the ordering of the Higgs bosons the same) except those involving  $H_3^0$ , which do not change sign. Two examples are  $H_5^0 H_3^+ W^-: -c_H/\sqrt{3}$ ; but  $H_3^0 H_5^+ W^-: -c_H$ .

Before turning to other couplings of interest, it is useful to reinterpret some of the features of Eqs. (2.14) and (2.15) in terms of  $J^{PC}$  quantum number assignments for the Higgs bosons. The discussion is closely analogous to that for the two-doublet model discussed in Ref. 1. Of course, all the Higgs bosons have  $J=0$ . Since the model conserves  $P$  and  $C$  in the absence of quarks and leptons, specific assignments are possible for  $P$  and  $C$  when considering only the Higgs- and vector-boson sectors of the theory. First, for this sector of the theory  $P=+$  for all Higgs bosons. Then, the absence of  $H_3^0 VV$  couplings in Eq. (2.14) can be reinterpreted as being equivalent to the assignment of  $C=-1$  to  $H_3^0$ . That is  $H_3^0$  is  $CP$  odd. As discussed in Ref. 1, this is easily understood physically, since  $H_3^0$  is the combination of imaginary parts of fields that is orthogonal to the Goldstone boson  $G_3^0$  [see Eqs. (2.6) and (2.8)], and thus will have the same  $CP$  assignment.  $G_3^0$  being derivatively coupled to the  $Z$  must have  $C=-1$  and  $P=+$ . From Eq. (2.8), we see that the  $H_3^0$ ,  $H_1^0$ , and  $H_1^{0'}$  are all combinations of the real parts of the Higgs fields. From the covariant derivative structure of  $\mathcal{L}_{\text{kin}}$  in Eq. (2.2), they develop nonzero  $VV$  couplings by virtue of the fact that the vacuum expectation values are chosen to be real. These nonzero couplings obviously require the assignment  $C=+1$  for all three of these neutral Higgs bosons. Finally, we note that when fermions are introduced into the model,  $C$  and  $P$  are no longer separately conserved (see Ref. 1 for a discussion in the context of the two-doublet model), but  $CP$  remains a good quantum number.

The  $Z$  couplings to a pair of neutral Higgs bosons exhibited in Eq. (2.15) are easily understood in terms of the above  $CP$  assignments. Since the  $Z$  has even  $CP$ , and since the coupling to two spin-zero Higgs bosons is a  $P$  wave, one of the neutral Higgs bosons must have even  $CP$  and the other must have odd  $CP$  (i.e., must be the  $H_3^0$ ).

Let us now turn to the self-couplings of the Higgs bosons. In order to compute these, we must precisely specify the potential for the Higgs sector. We adopt the form given in Ref. 5. It is the most general form of the Higgs sector potential subject to the requirements that it preserve the custodial  $SU(2)$  and that it be invariant under  $\chi \rightarrow -\chi$ . The latter requirement is imposed for the sake of simplicity, in order to eliminate cubic terms in the potential, but we believe that it does not significantly alter the phenomenology of the model. In our notation the potential is written as

$$\begin{aligned}
V_{\text{Higgs}} &= \lambda_1 (\text{Tr} \phi^\dagger \phi - c_H^2 v^2)^2 + \lambda_2 (\text{Tr} \chi^\dagger \chi - \frac{3}{8} s_H^2 v^2)^2 + \lambda_3 (\text{Tr} \phi^\dagger \phi - c_H^2 v^2 + \text{Tr} \chi^\dagger \chi - \frac{3}{8} s_H^2 v^2)^2 \\
&\quad + \lambda_4 \left[ \text{Tr} \phi^\dagger \phi \text{Tr} \chi^\dagger \chi - 2 \sum_{ij} \text{Tr} (\phi^\dagger \tau_i \phi \tau_j) \text{Tr} (\chi^\dagger t_i \chi t_j) \right] + \lambda_5 [3 \text{Tr} (\chi^\dagger \chi \chi^\dagger \chi) - (\text{Tr} \chi^\dagger \chi)^2],
\end{aligned} \tag{2.17}$$

where the  $\phi$  and  $\chi$  fields were defined in Eq. (2.1), the  $\tau_i$  are the usual Pauli matrices, and the  $t_i$  are the SU(2)-triplet representation matrices in the convention of Ref. 3. From this potential we obtain the Higgs-boson masses and couplings.

As stated earlier, all members of the fiveplet have the same mass as do all members of the threeplet. These masses are

$$m_{H_5}^2 = 3(\lambda_5 s_H^2 + \lambda_4 c_H^2)v^2, \quad m_{H_3}^2 = \lambda_4 v^2. \quad (2.18)$$

In general, the  $H_1^0$  and  $H_1^{0'}$  can mix according to the mass-squared matrix

$$\mathcal{M}_{H_1^0, H_1^{0'}}^2 = \begin{pmatrix} 8c_H^2(\lambda_1 + \lambda_3) & 2\sqrt{6}s_H c_H \lambda_3 \\ 2\sqrt{6}s_H c_H \lambda_3 & 3s_H^2(\lambda_2 + \lambda_3) \end{pmatrix} v^2. \quad (2.19)$$

Clearly, the mixing between  $H_1^0$  and  $H_1^{0'}$  vanishes in the limit of  $\lambda_3 \rightarrow 0$ . In this limit, there are only four Higgs potential parameters and the four independent Higgs-boson masses can be used to determine them uniquely. More generally, specifying the masses of the four Higgs-boson-mass eigenstates leaves one undetermined parameter in the potential.

It is worth noting that, even though a nonzero vacuum expectation value for  $\chi^0$  explicitly violates the U(1) symmetry associated with lepton number [when we introduce the couplings of Eq. (2.9)], there is no zero-mass Goldstone boson associated with this spontaneous breaking. This is because the  $\lambda_4$  term of the Higgs potential contains terms which explicitly violate lepton-number conservation when  $L = -2$  is assigned to the  $\chi$  fields but  $L = 0$  to all other Higgs fields. Thus, as long as  $\lambda_4 \neq 0$  we find  $m_{H_3}^2 \neq 0$ , in contrast with the situation in the Gelmini Roncadelli model<sup>8</sup> where no explicit lepton-number violation is introduced.

From the above results for the Higgs-boson masses, we see that if all the  $\lambda_i$  are similar in magnitude and  $s_H \rightarrow 0$  (implying that the doublet field is primarily responsible for the  $W$  and  $Z$  masses), then the lightest Higgs boson is predominantly composed of  $H_1^{0'}$ , a mixture of triplet fields. In the other extreme,  $c_H \rightarrow 0$  (implying that the triplet fields are responsible for giving the  $W$  and  $Z$  their mass) and the lightest Higgs boson is predominantly  $H_1^0$ , the real part of the neutral doublet field. This is clearly an amusing systematic structure, in that the lightest Higgs boson is always the one that has the least to do with the symmetry-breaking mechanism. As we shall discuss later, it also means that unitarity requirements for the  $VV$  scattering processes impose significant constraints upon the model parameters.

Turning to the Higgs self-couplings, we will present only those (trilinear) couplings that are of immediate phenomenological interest in determining the decay patterns of the various Higgs bosons. Because of the mass degeneracy among the members of the fiveplet and among the members of the threeplet, the only (two-body) decays that might occur will be to channels containing two Higgs bosons not in the same multiplet as the decaying Higgs boson. This allows a very natural organization for the interesting couplings. In particular, any threeplet member

always couples to another threeplet, so that decays of a threeplet member to a pair of Higgs bosons are not kinematically allowed. Only the fiveplet members and  $H_1^0$  and  $H_1^{0'}$  can decay to a pair of Higgs bosons. We first give the relevant couplings for the fiveplet decays. We define the quantity  $\bar{\lambda}_{45} \equiv \lambda_4(\frac{4}{3} - s_H^2) - \lambda_5 c_H^2$ . Note that  $\bar{\lambda}_{45}$  is determined given a value for  $t_H \equiv \tan\theta_H$  and the masses  $m_{H_5}$  and  $m_{H_3}$  [see Eq. (2.18)]. The Feynman rules for the couplings are (to be multiplied by  $i$ )

$$\begin{aligned} H_5^+ + H_3^- H_3^- &= H_5^- - H_3^+ H_3^+ : -3\sqrt{2}s_H \bar{\lambda}_{45} v, \\ H_5^0 H_3^- H_3^+ &: -\sqrt{3}s_H \bar{\lambda}_{45} v, \\ H_5^+ H_3^- H_3^0 &= -H_5^- H_3^+ H_3^0 : 3s_H \bar{\lambda}_{45} v, \\ H_5^0 H_3^0 H_3^0 &: 2\sqrt{3}s_H \bar{\lambda}_{45} v. \end{aligned} \quad (2.20)$$

Notice that all these couplings, and hence the associated decay widths, are largest when  $s_H \rightarrow 1$ , i.e., when the triplet fields are responsible for electroweak symmetry breaking (EWSB). The other interesting couplings are those of the  $H_1^0$  and  $H_1^{0'}$ . Should the  $H_1^0$  and  $H_1^{0'}$  mix with one another, then it would be necessary to rotate the couplings presented to the correct mass eigenstate basis. For this reason, we present also the self-couplings of these two Higgs bosons. The relevant nonzero Feynman vertices are specified below (each must be multiplied by a factor of  $i$ ):

$$\begin{aligned} H_1^0 H_1^0 H_1^0 &: -24c_H(\lambda_1 + \lambda_3)v, \\ H_1^0 H_1^{0'} H_1^{0'} &: -8c_H \lambda_3 v, \\ H_1^0 H_1^0 H_1^{0'} &: -2\sqrt{6}c_H \lambda_3 v, \\ H_1^{0'} H_1^{0'} H_1^{0'} &: -6\sqrt{6}s_H \lambda_3 v, \\ H_1^0 H_3^0 H_3^0 &= H_1^0 H_3^+ H_3^- : 8c_H(s_H^2 \lambda_1 + \lambda_3 + \lambda_4)v, \\ H_1^0 H_5^0 H_5^0 &= H_1^0 H_5^+ + H_5^- - - H_1^0 H_5^+ H_5^- : \\ &\quad -8c_H(\lambda_3 + \lambda_4)v, \\ H_1^{0'} H_3^0 H_3^0 &= H_1^{0'} H_3^+ H_3^- : 2\sqrt{6}s_H(c_H^2 \lambda_2 + \lambda_3 + \frac{2}{3}\lambda_4)v, \\ H_1^{0'} H_5^0 H_5^0 &= H_1^{0'} H_5^+ + H_5^- - \\ &= -H_1^{0'} H_5^+ H_5^- : -2\sqrt{6}s_H(\lambda_2 + \lambda_3 + \lambda_5)v. \end{aligned} \quad (2.21)$$

Of course, the above  $S$ -wave couplings are fully consistent with  $CP$ -odd assignment for the  $H_3^0$ . For instance,  $H_3^0 H_3^+ H_3^-$  is forbidden since  $CP$  for the  $H_3^+ H_3^-$  pair must be even. Similarly,  $H_3^0 H_3^0 H_3^0$  is forbidden, as is  $H_3^0 H_5^0 H_5^0$ , whereas  $H_5^0 H_5^0$ , whereas  $H_5^0 H_3^0 H_3^0$  is allowed.

### III. NATURALNESS ISSUES

Just as in the standard model, there are quadratically divergent contributions to the Higgs-boson mass squared arising at one loop from diagrams containing gauge and Higgs bosons. This leads to the well-known hierarchy problem: namely, how to understand why the Higgs boson(s) should be relatively light (as required by tree-level unitarity, see next section) when the only cutoff for such divergences in a grand unification scenario would be

expected to be very large. In the present model, there is an additional hierarchy problem arising from the breaking of the custodial  $SU(2)_R$  by interactions of the Higgs fields with the  $B$  gauge field (as mentioned in the previous section). At the one-loop level, this gives rise to quadratically divergent contributions both to  $\rho-1$  and to certain mixings among the Higgs bosons and between the Higgs bosons and the gauge fields. For instance, a phenomenologically important set of mixings which exhibit such divergences are those between the  $H_5^+$  and the  $H_3^+$  Higgs field, the  $W^+$ , and (in Feynman gauge) the  $G_3^+$  Goldstone boson. In contrast, charge conservation forbids mixings for the  $H_5^+$ , while explicit one-loop computations reveal that the  $H_5^0$  can mix with the  $H_1^0$ , but cannot mix with the  $H_3^0$ ,  $Z$ , or  $G_3^0$ . These latter mixings are zero at one loop by virtue of cancellations among various nonzero diagrams. This result, and the coupling symmetries necessary for this cancellation, are required by the  $CP$ -even assignment of the  $H_5^0$ , as opposed to the  $CP$ -odd quantum numbers for the  $H_3^0$ ,  $Z$ , and  $G_3^0$ , outlined in the previous section. Indeed, a renormalizable theory cannot require the introduction of counterterms in the fundamental Lagrangian that violate the  $CP$  properties of the theory. By the same reasoning, mixings of the  $H_1^{0'}$  with the  $H_3^0$ ,  $Z$ , and  $G_3^0$  are zero. Of course, there is a mixing of  $H_1^{0'}$  with  $H_1^0$ ; such mixing is present even at the tree level if  $\lambda_3 \neq 0$ . Returning to  $\rho-1$ , the  $H_5^+$  mixings, and the  $H_5^0$ - $H_1^0$  mixing, since they are quadratically divergent it would be most natural to expect them to be large in the context of a simple grand unified theory (GUT) where such divergences are cut off only by the large GUT scale.

Solutions to the mass hierarchy problem, such as supersymmetry, are undoubtedly just as viable as in the case of Higgs-doublet sector models. They would presumably also act to make the custodial  $SU(2)_R$  breaking small. However, we shall not attempt to explicitly construct a supersymmetric version of the Higgs-triplet model here. Instead, we shall adopt an approach analogous to that used in exploring the simplest one-doublet standard-model Higgs sector. Namely, we simply fine-tune our Higgs potential in such a way that Higgs-boson masses and  $SU(2)_R$  breaking at one loop are sufficiently small that tree-level perturbative results are generally reliable. For instance, if at one loop one allows  $SU(2)_R$  breaking in the Lagrangian, especially the Higgs potential, then it is possible to introduce appropriate counterterms to cancel the infinite parts of  $\rho-1$ ,  $H_5^+-H_3^+$  mixing,  $H_5^+-W^+$  mixing,  $H_5^+-G_3^+$  mixing, and  $H_5^0$ - $H_1^0$  mixing and render the finite remainders very small. Indeed, we can even choose to adjust the  $H_5^+$  and  $H_5^0$  mixings to be zero on the  $H_5$  mass shell; then, not only are the one-loop contributions to  $\rho-1$  finite, there is no residual quadratic dependence of  $\rho-1$  on the Higgs-boson masses (i.e.,  $\rho-1$  is shielded as in the SM).

The main phenomenological sensitivity to this issue arises in considering the fermion-antifermion couplings of the  $H_5^+$  and  $H_5^0$  that first arise through one-loop diagrams.<sup>9</sup> If the above mixings of the  $H_5^+$  and  $H_5^0$  are fine-tuned to zero or, at least, kept as small as is typical of finite one-loop corrections, their fermion-antifermion

couplings need only be considered when tree-level two-body decays are kinematically disallowed. In later sections we shall briefly outline the likely affects of small one-loop-induced couplings. A thorough treatment of these fine-tuning issues will appear in a separate paper.

#### IV. CONSTRAINTS FROM UNITARITY AND WEAK INTERACTIONS

Constraints obtained by requiring that scattering amplitudes for longitudinally polarized vector bosons not exceed unitarity limits have provided important guidelines on possible Higgs-boson masses in both the standard model and in many nonminimal Higgs scenarios.<sup>1</sup> We shall see that the present model is no exception. Weak-interaction experiments can also provide constraints. This is because the magnitude of  $B$ - $\bar{B}$  mixing can be strongly affected by a charged Higgs boson that couples to fermion-antifermion channels.<sup>1</sup> By combining experimental information on  $B$ - $\bar{B}$  mixing with the well-established measurements of  $\epsilon_K$  in  $K$ - $\bar{K}$  mixing and with recent results on the ratio of  $b \rightarrow u$  to  $b \rightarrow c$  decays, significant constraints on the  $H_3^+$  can be obtained.<sup>10</sup>

##### Unitarity

It is both amusing and useful to examine the manner in which high-energy unitarity is preserved for longitudinal vector-boson scattering processes in this model. For Higgs-sector extensions involving only doublets and singlets good high-energy behavior for longitudinal vector-boson scattering is guaranteed if  $\sum_i g_{h_i^0 VV}^2 = g_{\phi^0 VV}^2$ , where  $i$  runs over all neutral Higgs bosons of the nonminimal model, and  $\phi^0$  is our notation for the standard model Higgs boson. However, the manner in which good high-energy behavior is obtained in Higgs-sector extensions containing triplets and higher representations is much more complicated.<sup>11</sup> We give two examples in the context of the model being discussed in this paper. Consider  $ZW^- \rightarrow ZW^-$ . In the SM there is one  $t$ -channel graph involving the exchange of the  $\phi^0$ , with effective strength proportional to  $g^2 m_Z^2$ . In our triplet model the couplings of Eq. (2.14) make it clear that we have three  $t$ -channel graphs for the neutral Higgs bosons, and an  $s$ -channel and a  $u$ -channel graph for the singly charged  $H_5^-$ . The latter  $s$ - and  $u$ -channel graphs combine together to give the same result as a  $t$ -channel graph except for an overall sign difference. Thus, the four contributions have effective strength proportional to

$$\begin{aligned} H_1^0: & g^2 c_H^2 m_Z^2, \\ H_1^{0'}: & \frac{8}{3} g^2 s_H^2 m_Z^2, \\ H_5^0: & -\frac{2}{3} g^2 s_H^2 m_Z^2, \\ H_5^-: & -g^2 s_H^2 m_Z^2, \end{aligned} \tag{4.1}$$

where the minus sign in the  $H_5^-$  case is introduced to account for the sign difference alluded to above. Clearly the sum of all four terms gives back the original  $g^2 m_Z^2$  of the SM Higgs  $t$ -channel-exchange graph. However, a

nonzero vertex for  $W^- H_5^+ Z$  was crucial. Such a vertex cannot appear in a multidoublet model, and this is why the unitarity sum rule takes a much simpler form in such models. It is also amusing to consider the case of  $W^+ W^+ \rightarrow W^+ W^+$  scattering. In the SM there are two  $\phi^0$ -exchange graphs: One is a  $t$ -channel and the other a  $u$ -channel graph. They can be thought of as combining together and having effective strength  $g^2 m_W^2$ . In our triplet model we have three  $t$ -channel and three  $u$ -channel neutral Higgs graphs, and an  $s$ -channel graph, the latter involving the  $H_5^{++}$ . An  $s$ -channel graph is equivalent to the sum of a  $t$ - and  $u$ -channel graph except for an overall sign. Thus the effective strengths of the various contributions are

$$\begin{aligned} H_1^0: & g^2 c_H^2 m_W^2, \\ H_1^{0r}: & \frac{8}{3} g^2 s_H^2 m_W^2, \\ H_3^0: & \frac{1}{3} g^2 s_H^2 m_W^2, \\ H_5^{++}: & -2g^2 g_H^2 m_W^2, \end{aligned} \quad (4.2)$$

and again these sum to give the SM result.

Now that we have understood the manner in which good high-energy behavior for amplitudes involving longitudinally polarized vector bosons is guaranteed, we can turn to approximate numerical constraints imposed upon Higgs-boson masses by requiring that they be small enough that the various tree-level scattering amplitudes never numerically exceed their unitarity limits. We first recall that in the SM the mass of the  $\phi^0$  must be below roughly 1 TeV (Ref. 12) in order that  $WW$ ,  $ZZ$ ,  $\phi^0 Z$ , and  $\phi^0 \phi^0$  coupled channel tree-level scattering amplitude matrix not violate the  $S$ -wave unitarity bound in the  $s \rightarrow \infty$  limit.<sup>13</sup> If we combine this fact with the pattern of Higgs boson masses discussed below Eq. (2.19), and with the amplitude contributions outlined in Eqs. (4.1) and (4.2), it is easy to state the general constraints which emerge in the extreme limits of  $\tan\theta_H \rightarrow 0$  and  $\tan\theta_H \rightarrow \infty$ . In the first case,  $c_H \rightarrow 1$  and Eqs. (4.1) and (4.2) show that  $m_{H_1^0}$  plays the role of the SM Higgs boson, and must have mass below  $\sim 1$  TeV. *A priori*, in this  $c_H = 1$  case, the other Higgs bosons are not constrained by unitarity requirements and they could be quite heavy. However, Eqs. (2.19) makes it clear that  $m_{H_1^{0r}}$  is in fact much smaller than  $m_{H_1^0}$  as long as there are no unnaturally large ratios among the  $\lambda_i$ . Further, the other Higgs-boson masses squared are also related to  $m_{H_1^0}^2$  [see Eq. (2.18)]:

$$m_{H_1^0}^2 : m_{H_5^0}^2 : m_{H_3^0}^2 = 8(\lambda_1 + \lambda_3) : 3\lambda_4 : \lambda_4. \quad (4.3)$$

Again assuming all  $\lambda_i$  are similar in size, we see that the  $H_5^0$  is likely to be significantly lighter than the  $H_1^0$  and the  $H_3^0$  could easily be lighter still. In the other extreme of  $s_H \rightarrow 1$ , Eqs. (4.1) and (4.2) imply that  $m_{H_1^{0r}}$  and  $m_{H_5}$  should both lie below roughly 1 TeV. Note, in particular, that the couplings are such that even if one of these two masses is small, there is no possibility for the unitarity bound on the other mass to be weakened.<sup>14</sup> In this  $s_H = 1$

case,  $m_{H_1^0}$  and  $m_{H_5}$  are not constrained by unitarity in vector-boson scattering. However, the  $H_1^0$  mass is most naturally much smaller than  $m_{H_1^{0r}}$  in the  $s_H \rightarrow 1$  limit according to Eq. (2.19), and using Eq. (2.18) we also have the ratios

$$m_{H_1^{0r}}^2 : m_{H_5^0}^2 : m_{H_3^0}^2 = 3(\lambda_2 + \lambda_3) : 3\lambda_5 : \lambda_4. \quad (4.4)$$

From this equation we conclude that  $m_{H_5}$  is most naturally somewhat smaller than  $m_{H_1^{0r}}$ , while  $m_{H_3}$  could easily be smaller still. For middle of the road  $\tan\theta_H$  values,  $H_1^0$ ,  $H_1^{0r}$ , and the various  $H_5$ 's all contribute to vector-boson scattering amplitudes. The contributions are such that all must be lighter than  $\sim 1$  TeV. Equation (2.18) implies that  $m_{H_3}$  will be smaller than this if the  $\lambda_i$ 's are all similar in size. The most important overall conclusion is obvious. Barring extreme and (hence) unnaturally large ratios among the  $\lambda_i$ , none of the Higgs bosons of this model can be extremely heavy if unitarity for  $W^+ W^-$ , . . . is to be obeyed at the tree level for all energies. They should all lie in the 1-TeV mass range or below. In addition, we always find that some mixture of  $H_1^0$  and  $H_1^{0r}$  is likely to be substantially lighter than the other Higgs bosons.

#### Weak-interaction constraints

The constraints upon a charged Higgs boson deriving from  $B$ - $\bar{B}$  mixing depend upon the strength of the  $H^- t\bar{b}$  coupling. The physics behind such constraints is reviewed in Ref. 1, in the case of the charged Higgs boson of a two-doublet model. A recent analysis appears in Ref. 10. The results and graphs of the latter treatment are presented in terms of the charged-Higgs-boson mass and a parameter  $\tan\beta$  whose inverse ( $\cot\beta$ ) determines the strength of the term proportional to  $m_t$  in the  $H^- t\bar{b}$  coupling. Comparing the coupling employed there to that given in Eq. (2.13) for  $H_3^- t\bar{b}$ , we see that all results of Ref. 10 apply with the replacement  $\cot\beta \rightarrow \tan\theta_H$ . We do not go into details here, but summarize the conclusions. First, we recall that the resulting constraints are imprecise for four important reasons: (i) The amount of  $B$ - $\bar{B}$  mixing as extracted from existing data has a large experimental error; (ii) the hadronic-matrix-element factors that enter into computing  $\epsilon_K$  and  $B$ - $\bar{B}$  mixing have not yet been determined precisely, (iii) the  $b \rightarrow u/b \rightarrow c$  decay ratio has a large experimental error; and, perhaps most crucially, (iv) we do not know the value of  $m_t$ . While there is still a significant possibility that we have not observed the top because of the dominance of decay modes involving a charged Higgs boson (in the present model  $t \rightarrow H_3^+ \bar{b}$ , followed by  $H_3^+ \rightarrow c\bar{s}, \tau^+ \nu, \dots$ ) it is most likely that the top quark really is heavier than the  $\sim 70$ -GeV limits that are extracted (ignoring the above mode) from current hadron collider data. Let us assume that  $m_t \sim 80$  GeV and that experimental measurements of  $\epsilon_K$ ,  $B$ - $\bar{B}$  mixing, and  $b \rightarrow u/b \rightarrow c$  are within 2 standard deviations of the correct result. If we adopt (within reasonable theoretical error bars) hadronic-matrix-element factor

values allowing maximum room for a charged Higgs boson, then a few benchmark constraints can be stated: (1)  $\tan\theta_H > 10$  would require  $m_{H_3} \gtrsim 1$  TeV, in conflict with our earlier unitarity discussion; (2)  $\tan\theta_H > 5$  is only possible for  $m_{H_3} \gtrsim 100$  GeV; and (3)  $\tan\theta_H \lesssim 2.5$  allows any  $m_{H_3}$  value. Of course, for larger top-quark masses or middle-of-the-road values of the hadronic-matrix-element factors, the constraints are much stronger. For example, using moderate hadronic-matrix-element values,  $m_t \sim 160$  GeV would require  $m_{H_3} \gtrsim 1$  TeV for  $\tan\theta_H > 5$  and only  $\tan\theta_H \lesssim 1.5$  allows all  $m_{H_3}$  values to be consistent with the  $\epsilon_K$ ,  $B$ - $\bar{B}$  mixing, and  $b \rightarrow u/b \rightarrow c$  experimental results.

### Summary remarks on constraints

While we will not pay strict attention to the above constraints in all our phenomenological analyses, they should clearly be used as guidelines to determine the most likely regions of parameter space for this model. Certainly, we should not consider Higgs-boson masses above 1 TeV, nor  $\tan\theta_H$  values above 10, with  $\tan\theta_H \lesssim 1.5$  and  $m_{H_3} \gtrsim m_W$  being strongly preferred (so long as we believe  $m_t \gtrsim 80$  GeV).

### V. HIGGS-BOSON DECAYS

The manner in which the Higgs bosons of the model decay is, of course, critical in determining what signatures to use in searches for them. The decays of the Higgs bosons of this model exhibit many ‘‘abnormalities’’ compared to the decay patterns of a standard-model Higgs boson. We have already noted that the fiveplet members, as well as the  $H_1^{0'}$ , do not have any tree-level  $f\bar{f}$  couplings, while the triplet bosons have no tree-level  $VV$  ( $V=W$  or  $Z$ ) couplings. In addition, all the Higgs bosons of the model have  $HV$  ( $H$  stands for any Higgs boson) and  $HH$  couplings. We shall find that the resulting Higgs-boson-decay modes are typically very important when allowed. In order to gain an understanding of the most likely patterns for decay of each of the Higgs bosons, we shall present a series of graphs illustrating the relative importance of various modes as a function of the mass of the decaying Higgs boson, for fixed masses of the other Higgs bosons and for several values of  $\tan\theta_H$  (0.1, 1.5, and 10). In discussing  $H_1^0$  and  $H_1^{0'}$ , we shall consider the extreme of  $\lambda_3 \simeq 0$ , corresponding to small mixing between these two singlets. This limit gives the largest difference between their decays. In addition, from Eqs. (2.18) and (2.19), we see that it allows us to determine all four remaining  $\lambda_i$ , and hence all Higgs trilinear couplings, in terms of the masses  $m_{H_1^{0'}}$ ,  $m_{H_1^{0'}}$ ,  $m_{H_3}$ , and  $m_{H_5}$ .

The decays of the  $H_3$  bosons are the most easily discussed. We present results for  $H_3^+$  and  $H_3^0$  in Figs. 1 and 2, respectively. For the triplet members, the only allowed channels are fermion-antifermion and  $HV$  channels.  $HH$  channels are kinematically forbidden because of the degeneracy of the triplet members and because of the fact

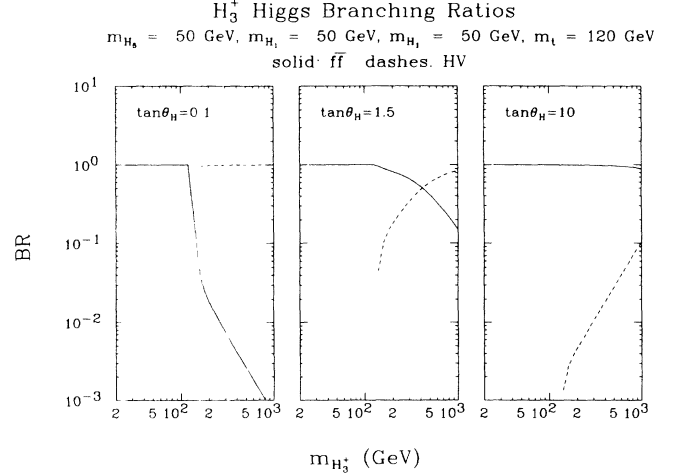


FIG. 1. Branching ratios for  $H_3^+$  decays to  $f\bar{f}'$  (solid line), and  $HV$  (dashed line) channels. See text for further details.

that every triplet member must couple to another triplet member in the Higgs trilinear couplings. Further, we have already noted the absence of  $VV$  couplings for triplet members. We plot only the fermion-antifermion branching ratio after summing over all channels (though, of course, the channel with the largest allowed masses dominates), and the net  $HV$  branching ratio after summing over all such channels. For the  $H_3^+$ , the possible  $HV$  channels are  $H_1^0 W^+$ ,  $H_1^{0'} W^+$ ,  $H_5^0 W^+$ , and  $H_5^+ Z$ . For the  $H_3^0$  the possible  $HV$  channels are  $H_1^0 Z$ ,  $H_1^{0'} Z$ ,  $H_5^+ W^-$ ,  $H_5^- W^+$ , and  $H_5^0 Z$ . Which channels of this type are allowed, of course, depends upon the Higgs- and vector-boson masses. We have chosen  $m_{H_5} = m_{H_1^{0'}} = m_{H_1^0} = 50$  GeV in order to exhibit just how important the  $HV$  modes can be when kinematically allowed. The only uncertainty regarding the fermion modes arises from the unknown mass of the top quark.

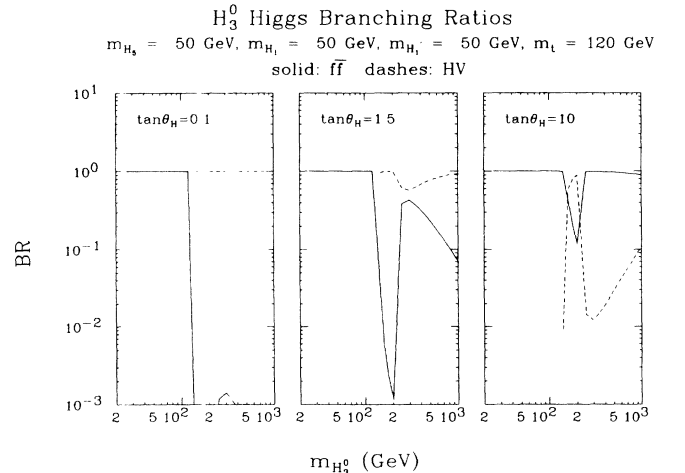


FIG. 2. Branching ratios for  $H_3^0$  decays to  $f\bar{f}$  (solid line), and  $HV$  (dashed line) channels. See text for further details.



We have arbitrarily taken  $m_t = 120$  GeV for our plots.

A few features of these results are noteworthy. In the case of the  $H_3^+$ , note that even though the  $t\bar{b}$  channel opens up at about the same  $m_{H_3}$  value as do the  $HV$  channels (for the particular mass choices we have made), it requires large  $\tan\theta_H$  (yielding enhanced  $f\bar{f}'$  couplings) in order to dominate. The importance of  $HV$  channels is even more evident in the  $H_3^0$  plots, where we see that below  $t\bar{t}$  threshold, the  $HV$  branching ratio is nearly 1 once the  $HV$  channels are kinematically allowed. Thus, when  $HV$  channels are open and  $\tan\theta_H$  is not large (as preferred on the basis of the weak-interaction constraints discussion) the signatures for the  $H_3$  Higgs bosons will typically be quite complex, being determined by the well-known two-body decay modes of the  $W$  and  $Z$  and the decays modes of the other Higgs bosons that we shall discuss shortly. Regarding the latter, for now we only note that, when light, the  $H_1^0$  has  $f\bar{f}$  decay modes, while  $H_1^{0'}$  and the  $H_5$ 's can have more complicated decays. Thus, it is important to know which type of  $H$  dominates in the  $HV$  modes. The pattern is easily specified. When  $\tan\theta_H = 0.1$  the  $H_1^0 V$  modes (in both  $H_3^0$  and  $H_3^+$  decays) are very small compared to the others. When  $\tan\theta_H = 1.5$  the  $H_1^0 V$  modes are similar in importance to other  $HV$  modes. And when  $\tan\theta_H = 10$ , the  $H_1^0 V$  channels are by far the most important of the  $HV$  modes. These systematics are, of course, a direct result of the fact that the  $H_3^0 H_1^0 V$  couplings are proportional to  $s_H$ , while the others are proportional to  $c_H$  [see Eq. (2.15)].

It is useful to consider next the  $H_1^0$  decays. Like the  $H_3$  bosons, the  $H_1^0$  has tree-level fermion-antifermion couplings. However, the list of alternative channels is far more complex, including  $VV$  channels ( $WW$  and  $ZZ$ ),  $HV$  channels ( $H_3^0 Z$ ,  $H_3^+ W^-$ , and  $H_3^- W^+$ ; couplings to  $H_5^+ W^-$ ,  $H_5^-$ ,  $H_5^- W^+$ , and  $H_5^0 Z$  are zero), and  $HH$  channels ( $H_3^0 H_3^0$ ,  $H_3^+ H_3^-$ ,  $H_5^0 H_5^0$ ,  $H_5^+ H_5^-$ , and  $H_5^{++} H_5^{--}$ ). Results for  $m_{H_5} = m_{H_3} = m_{H_1^{0'}} = 50$  GeV (Ref. 15) and  $m_t = 120$  GeV are given in Fig. 3. Again, we see that  $f\bar{f}$

modes only dominate when the other channels are not allowed. This, of course, is not unlike the situation for the SM Higgs boson where the  $VV$  channels are the most important when allowed. The new feature here is that the  $VV$  channels themselves are only dominant over the  $HV$  and  $HH$  channels when  $\tan\theta_H$  is very small. As  $\tan\theta_H$  increases, the  $HH$  modes become the largest category. This results in complicated signatures for the  $H_1^0$ . In fact, it is important to know how the  $HH$  modes are distributed between  $H_3 H_3$  versus  $H_5 H_5$  channels, since the  $H_3$  and  $H_5$  can have very different decays. We find that the  $H_3 H_3$  modes are by far the more important of the two, independent of  $\tan\theta_H$ . Since  $H_3$ 's that are less massive than  $m_W$  and  $m_Z$  decay to fermion-antifermion channels, we see that a possible signature for the  $H_1^0$  would involve a four-fermion final state. On the other hand, our discussion of constraints from weak interactions taught us that a light  $H_3$ -plet is only likely if  $\tan\theta_H$  is relatively small, so that this scenario is most probably only viable for  $\tan\theta_H \lesssim 1.5$ . If we choose  $m_{H_3}$  to be large, then the reader might wonder if the  $H_5 H_5$  modes can still dominate the  $f\bar{f}$ ,  $HV$ , and  $VV$  channels when  $H_3 H_3$  modes are kinematically forbidden. In fact, when kinematically allowed, the  $H_5 H_5$  modes are completely dominant (until the  $H_3 H_3$  modes open up). The reason is that large  $m_{H_3}$  implies large  $\lambda_4$  [Eq. (2.18)] which leads to large  $H_5^0 H_5^0$  couplings [Eq. (2.22)].

Let us now turn to the  $H_5$ -plet members and the  $H_1^{0'}$ . Since the  $H_5$ 's and (For  $\lambda_3 = 0$ ) the  $H_1^{0'}$  have no tree-level fermion-antifermion couplings, their decays exhibit many novel features. Indeed, the only possible tree-level couplings to fermions are to lepton-lepton channels through the interaction Lagrangian of Eq. (2.9). We shall shortly argue that these interactions are not likely to be important. Thus, we first outline the results obtained in their absence. In this case, the only tree-level decays of the  $H_5$ 's and  $H_1^{0'}$  are to virtual or real  $HV$ ,  $VV$ , or  $HH$  channels. In particular, when the  $H_5$ 's and  $H_1^{0'}$  are sufficiently light that neither of the bosons in the above channels are kinematically allowed to be on shell, i.e., both bosons are virtual (denoted as  $B^* B^*$  modes,  $B = H$  or  $V$ ), the tree-level mediated decay width can be very small. In this mass domain, one must consider the possibility that mixing or one-loop-induced  $f\bar{f}$  couplings are important. For the  $H_5^{++}$ , quantum numbers forbid  $f\bar{f}$  couplings to quarks and leptons to all orders. Thus, the decays of the  $H_5^{++}$  in this mass region are entirely of the  $B^* B^*$  type, resulting in four-body states with two nonresonant fermion-antifermion pairs. For the  $H_5^+$ ,  $H_5^0$ , and  $H_1^{0'}$  we must consider, as well, the mixing and/or one-loop induced decays. For instance, for the  $H_1^{0'}$  even a very small value for  $\lambda_3$  will induce significant mixing with the  $H_1^0$  and, thereby, non-negligible  $f\bar{f}$  couplings. In the case of the  $H_5^+$ ,  $f\bar{f}'$  couplings can arise via one-loop diagrams which mix the  $H_5^+$  with the  $H_3^+$ ,  $W^+$ , and  $G_3^+$  (all of which have fermion-antifermion couplings), as well as via triangle-type one-loop diagrams. Similarly,  $H_5^0$  couplings to  $f\bar{f}$  can be generated both by  $H_5^0 H_1^0$  mixing and by triangle loop diagrams. As noted earlier, although the one-

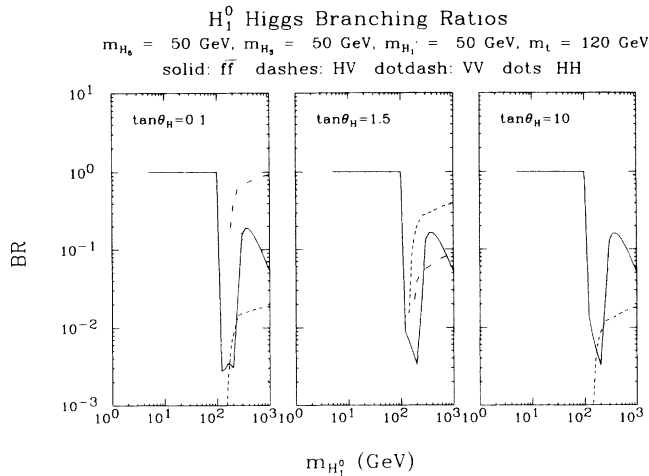


FIG. 3. Branching ratios for  $H_1^0$  decays to  $f\bar{f}'$  (solid line),  $HV$  (dashed line),  $VV$  (dotted-dashed line) and  $HH$  (dots) channels. See text for further details.

loop mixing diagrams are potentially infinite, fine-tuning can be performed to keep mixing-generated fermion-antifermion couplings at a level typical of (finite) one-loop-induced couplings found in other models (e.g., the standard model one-loop corrections to Higgs  $f\bar{f}$  couplings). Even if we were to fine-tune all such mixings to zero (a possibility), the (finite) triangle-diagram-induced couplings of the  $H_5^+$  and  $H_5^0$  to fermion-antifermion channels would remain. These finite triangle-diagram-induced fermion-antifermion couplings are also present for the  $H_1^{0'}$  (but probably unimportant compared to the  $\lambda_3 \neq 0$  mixing contributions for the latter). All of these one-loop effects will be considered in more depth in a later paper. For the present, we merely note that induced couplings of typical one-loop magnitude are likely to be sufficiently large that the fermion-antifermion channels dominate the decays of the  $H_5^+$ ,  $H_5^0$ , and  $H_1^{0'}$  whenever these Higgs bosons are so light that the only allowed decays using tree-level couplings are of the  $B^*B^*$  type in which *both* intermediate bosons in the  $VV$ ,  $HV$ , and  $HH$  channels must be virtual.

However, once the decaying  $H_5^+$ ,  $H_5^0$ , or  $H_1^{0'}$  has a mass large enough that at least one of the bosons in the  $VV$ ,  $HV$ , or  $HH$  channels can be on shell (denoted as  $BB^*$  channels), the loop-mediated  $f\bar{f}$  channel decay widths most probably are sufficiently small that the mixed real-virtual  $BB^*$  channels take over. (As we note shortly, this and related statements below must be modified for the  $H_1^{0'}$  if  $\lambda_3$  is not extremely small.) The exact point of cross over depends upon such details as the threshold locations of the  $BB^*$  channels and the exact size of the one-loop-induced couplings. Thus, there are three basic kinematical domains to consider in describing the decays of the  $H_5^+$ ,  $H_5^0$ , and  $H_1^{0'}$ : (i) The low-mass decay region where both of the intermediate bosons in the  $VV$ ,  $HV$ , and  $HH$  channels must be virtual and decays are dominated by loop-induced fermion-antifermion couplings, yielding  $f\bar{f}$  final states; (ii) an intermediate region where, for at least one of the  $VV$ ,  $HV$ , or  $HH$  channels one of the intermediate bosons can be real, but the other must be virtual—the crossover between loop-induced  $f\bar{f}$  decay modes and tree-level-induced  $BB^*$  channels most probably occurs in this region and, when the latter dominate, the final state consists of a real  $V$  or  $H$  plus an  $f\bar{f}$  pair; and (iii) the  $BB$  region where at least one of the  $VV$ ,  $HV$ , or  $HH$  two-body channels is kinematically allowed—loop-induced decays are negligible. Of course, in region (iii), and when the  $BB^*$  channels dominate in region (ii), we must ultimately consider how the  $H$  and  $V$  bosons decay—typically they will decay to an  $f\bar{f}$  final state. Thus, at low mass the  $H_5^+$ ,  $H_5^0$ , and  $H_1^{0'}$  will decay to a single  $f\bar{f}$  pair, while when  $BB^*$  or  $BB$  channels dominate the final state will contain *two*  $f\bar{f}'$  pairs.

In fact, because of the likelihood that  $\lambda_3 \neq 0$  and, therefore, that there will be some  $H_1^0$ - $H_1^{0'}$  mixing, the  $f\bar{f}$  couplings of the  $H_1^{0'}$  arising from the  $H_1^0 f\bar{f}$  couplings via this mixing can easily be larger than those coming from one-loop diagrams. In such a case, the  $f\bar{f}$  decay channels of the  $H_1^{0'}$  are likely to be dominant until the doubly on-shell  $BB$  decay channels are allowed. Thus, at low to

moderate mass the (slightly mixed)  $H_1^{0'}$  is most likely to decay to a single  $f\bar{f}$  pair, while at higher masses the final state will contain two  $f\bar{f}$  pairs.

In the case of the  $H_5^{++}$ , the only decay channels available at low mass are the  $B^*B^*$  channels, and the final states will *always* contain two  $f\bar{f}'$  pairs. As a result, it will have a very long lifetime at low mass.

Let us now consider in more detail the considerations appropriate when there are only tree-level couplings. This discussion will apply without modification in the case of the  $H_5^{++}$ , and applies to all but the one-loop- or mixing-induced decays of the  $H_5^+$ ,  $H_5^0$ , and  $H_1^{0'}$ . In the absence of these latter decays, all decays at low mass are to intrinsically four-body final states, via  $B^*B^*$  diagrams. In fact, for any of the Higgs bosons, the only  $B^*B^*$  diagrams of importance are the  $V^*V^*$  diagrams; the  $Hf\bar{f}$  couplings being proportional to  $m_f/m_W$  are much smaller than the  $Vf\bar{f}$  couplings, so that  $H^*$  diagrams are substantially suppressed in comparison.<sup>16</sup> The results we shall present are obtained keeping only the  $V^*V^*$  diagrams, but we have explicitly checked that these are indeed the dominant diagrams in several specific cases. For similar reasons, in the three-body region only  $VV^*$  and  $HV^*$  diagrams are important (although we have performed our calculations keeping all diagrams in the three-body cases). We note that our results are completely insensitive to the specific value of the top-quark mass as long as the  $t\bar{b}$  channel (in the case of the  $H_5^+$ ) and  $t\bar{t}$  channels (in the case of  $H_5^0$  and  $H_1^{0'}$ ) have mass above the lowest  $BB^*$  channel threshold.

Of the four Higgs bosons,  $H_1^{0'}$  is certainly the most complicated to discuss, given the large number of channels that must be considered. Thus, we focus first on  $H_5$ 's which have relatively few channels with nonzero couplings. In the three-body region we have only  $Vf\bar{f}$  and  $H_3f\bar{f}$  channels, while in the two-body region we have  $VV$ ,  $H_3V$ , and  $H_3H_3$  channels. Thus, for the  $H_5$ 's the only parameter other than  $m_t$  and  $m_{H_5}$  requiring specification is  $m_{H_3}$ . By specifying  $m_{H_3}$  we determine the location of all thresholds for these channels, and, in addition, the values of  $m_{H_5}$  and  $m_{H_3}$  determine  $\lambda_4$  and  $\lambda_5$  [see Eq. (2.18)], and hence all  $H_5H_3V$  couplings [see Eq. (2.20)].

In order to establish a point of comparison, we consider first the  $H_5^{++}$ , for which mixing or one-loop-induced  $f\bar{f}'$  decay channels are not present at any level. In the four-body region only  $W^{++}W^{++}$  diagrams are important. In the three-body region we have the possibilities of  $H_3^+W^{++}$  ( $H_3^+H_3^+$  contributions are much smaller), and  $W^+W^{++}$  (with negligible  $W^+H_3^+$ ).<sup>17</sup> Finally, the two-body modes include  $W^+W^+$ ,  $H_3^+W^+$ , and  $H_3^+H_3^+$ . In Fig. 4 we present the lifetime  $c\tau$  for the  $H_5^{++}$  as a function of  $m_{H_5}$ . We have chosen  $m_{H_3} = m_W$  for this plot (and  $m_t = 80$  GeV). For  $\tan\theta_H = 0.1$ , the  $VV$  coupling of the  $H_5$ 's is suppressed [see Eq. (2.14)], and  $c\tau$  can be very large, e.g.,  $c\tau \gtrsim 1$  cm for  $m_{H_5} \lesssim 12$  GeV. For moderate and large  $\tan\theta_H$  values, the  $VV$  coupling is near full strength, and  $c\tau \lesssim 1$  cm for  $m_{H_5} \gtrsim 6.5$  GeV. Thus, de-

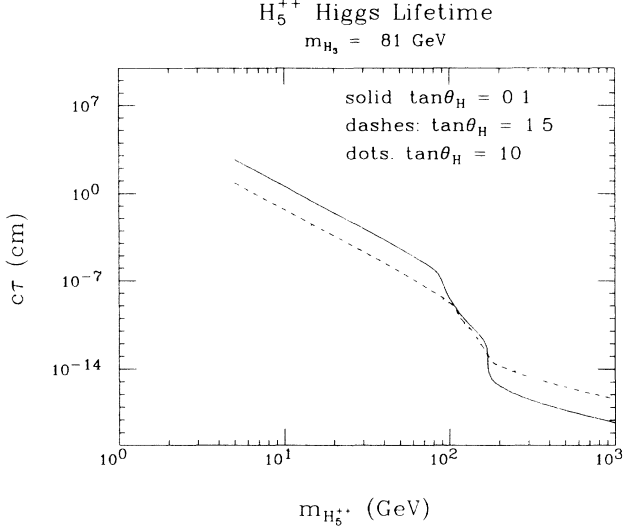


FIG. 4. The lifetime  $c\tau$  (in cm) of the  $H_5^{++}$  as a function of  $m_{H_5}$ . See text for details.

pending upon the appropriate boost factor and detector size, a light doubly charged  $H_5^{++}$  would appear as a heavily ionizing particle track either with or without a clearly separated decay vertex. As we shall review in more detail in the following section, the pair-production cross section for such an object is large at an  $e^+e^-$  collider, and it has certainly been ruled out up to and beyond the  $\sim 12$ -GeV benchmark mass value referred to above. As  $m_{H_5}$  increases, the  $H_5^{++}$  decay becomes prompt and only the two fermion-antifermion pairs emerging from the decay are visible. Since the invariant mass of the pairs will be weighted towards the maximum possible values, the resulting eight-fermion events would still provide a very distinctive signal at an  $e^+e^-$  collider, given the large  $H_5^{++}H_5^{--}$  pair production cross section. Thus, we believe that  $m_{H_5} \lesssim m_Z/2$  will shortly be ruled out by a combination of KEK Tristram, SLAC Linear Collider (SLC), and CERN data.

Once  $m_{H_5} \gtrsim \min[m_W, m_{H_3}]$ , the three-body decay channels open up, the lifetime drops rapidly, and two of the four final fermions coming from a single  $H_5^{++}$  will exhibit a mass peak at either  $m_W$  or  $m_{H_3}$ . The relative importance of the two modes, when both are allowed, is illustrated in Fig. 5. Since, the  $H_5VV$  couplings are proportional to  $s_H$ , while the  $H_5H_3V$  couplings are proportional to  $c_H$ , it is not surprising that the  $H_3f\bar{f}$  decay channels dominate at small  $\tan\theta_H$ , while the  $Vf\bar{f}$  channels dominate at large  $\tan\theta_H$ . The relative branching ratios of the various  $BB$  modes at large  $m_{H_5}$  are also given in Fig. 5. Once all two-body modes are allowed, the  $H_3H_3$  modes tend to dominate at small  $\tan\theta_H$ , while the  $VV$  modes are dominant at large  $\tan\theta_H$ ; the  $H_3V$  modes are never dominant. The reason for the dominance of  $H_3H_3$  modes at small  $\tan\theta_H$ , despite the relevant coupling being proportional to  $s_H$  [see Eq. (2.20)], is that  $\lambda_5$  must in general be large at small  $s_H$  in order to yield a

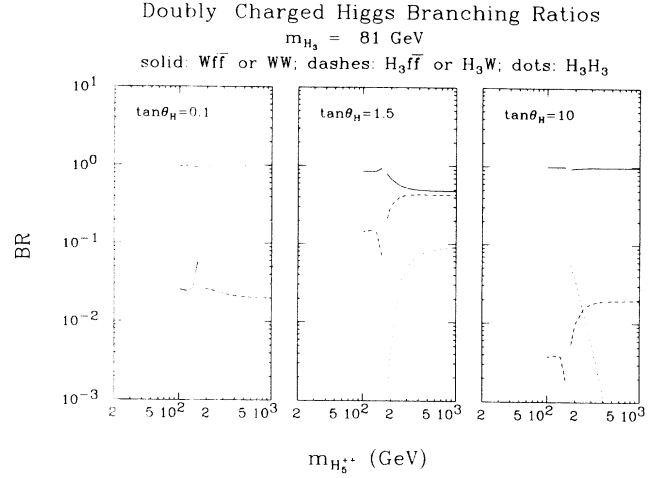


FIG. 5. Branching ratios for the  $H_5^{++}$  in the three-body and two-body regions. For parameter details see text.

predetermined  $m_{H_5}$  value [see Eq. (2.18)]. This leads to a very large  $\lambda_5 c_H^2$  term in  $\bar{\lambda}_{45}$  which controls the  $H_5H_3H_3$  couplings [see Eq. (2.20)].

What impact would  $H_5^{++} \rightarrow l^+l^+$  couplings have on these results? Using the limits on  $h_{ee}$  and  $h_{\tau\tau}$  given earlier (below Eq. (2.9)), and width of Eq. (2.12), we find

$$c\tau(H_5^{++} \rightarrow e^+e^+) \gtrsim \frac{1.5 \times 10^{10} s_H^2}{m_{H_5}(\text{GeV})} \text{ cm}, \quad (5.1)$$

$$c\tau(H_5^{++} \rightarrow \tau^+\tau^+) \gtrsim \frac{1.2 \times 10^{-5} s_H^2}{m_{H_5}(\text{GeV})} \text{ cm}.$$

Comparing to Fig. 4, we see that the restrictive  $\beta\beta_{0\nu}$  limits on  $h_{ee}$  imply that decays to  $e^+e^+$  are never important unless  $s_H^2$  is extremely small. Even if  $h_{\tau\tau}$  saturates its current upper limit,  $\tau^+\tau^+$  decays would only be dominant in the region where the only other decay mode is of the  $B^*B^*$  variety. ( $BB^*$  channels certainly dominate, once they open up.) Further, in the context of the present model, in which we imagine extending only the Higgs sector of the SM, it is most natural to suppose that *all* neutrinos are very light, and most probably massless, in which case the  $h_{ij}$  of Eq. (2.9) would be zero. Thus, we shall henceforth neglect these lepton-lepton decay channels.

Turning next to the  $H_5^+$ , we first make some further remarks on the competition between the tree-level-induced decay modes, and the  $f\bar{f}$  loop-induced decay modes. At low mass, the only  $V^*V^*$  diagram is  $W^{+*}Z^*$ . Possible  $BB^*$  modes include the  $Vf\bar{f}$  channels,  $ZW^{+*}$  (with a much smaller  $ZH_3^*$  contribution),  $W^{+*}Z^*$  (and small  $W^{+*}H_3^{0*}$ ); and the  $H_3f\bar{f}$  channels,  $H_3^+Z^*$  (and small  $H_3^+H_3^{0*}$ ), and  $H_3^0W^{+*}$  (and small  $H_3^0H_3^{+*}$ ). Finally in the  $BB$ -mode region, we have the  $VV$  channel  $W^+Z$ , the  $H_3V$  channels  $H_3^+Z$  and  $H_3^0W^+$ , and the  $H_3H_3$  channel  $H_3^+H_3^0$ . We present the lifetime  $c\tau$  of the  $H_5^+$ , computed for tree-level couplings only, in Fig. 6 as a function of

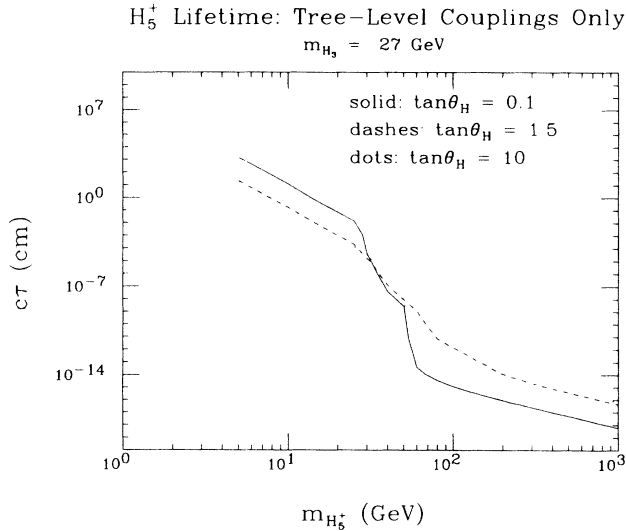


FIG. 6. The lifetime  $c\tau$  (in cm) of the  $H_5^+$  as a function of  $m_{H_5}$ . We plot  $c\tau$  computed by including only tree-level couplings. See the text for details and parameter specifications.

$m_{H_5}$ . We have taken  $m_{H_3} = 27$  GeV, in order to clearly distinguish  $HV$  from  $VV$  thresholds, and  $m_t = 80$  GeV. For small  $m_{H_5}$ , the  $c\tau$  obtained keeping only  $B^*B^*$  modes is somewhat greater than that for the  $H_5^{++}$  (because a virtual  $Z^*$  has weaker  $f\bar{f}$  couplings than does a  $W^{*+}$ ). For instance, at  $m_{H_5} = 5$  GeV, we have  $c\tau(H_5^+) \sim 2.8 - 3c\tau(H_5^{++})$  (depending on  $\tan\theta_H$ ).

However, we must now consider the  $f\bar{f}'$  couplings induced at one loop. As mentioned earlier, these will be considered in depth in another paper. Here, we simply summarize the results that obtain when they are finetuned (as described earlier) to a level typical of *finite* one-loop-induced effects. The  $c\tau$  obtained for the one-loop  $f\bar{f}'$  channels is such that they dominate the  $H_5^+$  decay width in the  $B^*B^*$  region. The crossover between the fermion-antifermion one-loop modes and the  $BB^*$ -type  $H_3f\bar{f}$  mode depends on details, but is typically a little above the threshold for the latter. Thus, we conclude that, as we vary the  $H_5^+$  mass, the  $f\bar{f}$  one-loop modes dominate until the  $BB^*$  modes open up, after which the tree-level-induced  $BB^*$  and  $BB$  modes are dominant—obviously, unlike the  $H_5^{++}$ , the  $H_5^+$  is never long-lived.<sup>18</sup> Thus, the searches for a light pair-produced charged Higgs boson that have been performed at the various  $e^+e^-$  colliders are completely relevant; existing limits and those expected from KEK Tristram, SLAC Linear Collider (SLC), and CERN and LEP will rule out the  $H_5^+$  if it has mass less than about  $m_Z/2$ .

Let us now examine in more detail the  $BB^*$  and  $BB$  decay regions. For this purpose, we take  $m_{H_3} = m_W$ . Besides being a reasonable value in light of the weak-interaction ( $B$ - $\bar{B}$  mixing) constraints reviewed earlier, this choice will allow us to compare  $HH$ ,  $HV$ , and  $VV$  modes throughout the  $m_{H_5}$  range where all might be present. Of course, if one or more is absent the other(s) become pro-

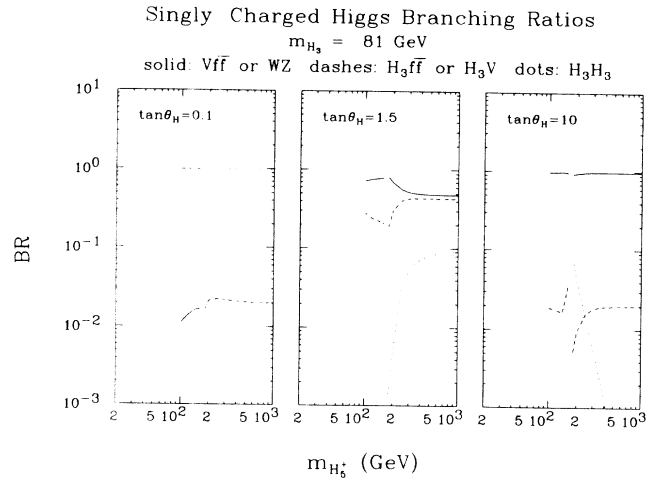


FIG. 7. Branching ratios for the  $H_5^+$  in the  $BB^*$  and  $BB$  decay regions. For details see text.

portionately larger. We present in Fig. 7 the branching ratios for the different types of channels. Obviously, the general patterns are extremely similar to those for the  $H_5^{++}$ .

The final member of the  $H_5$  multiplet is the  $H_5^0$ . For the  $B^*B^*$  modes, we have both  $W^{*+}W^{*-}$  and  $Z^*Z^*$  graphs to include. The  $BB^*$  channels include the  $Vf\bar{f}$  channels of  $ZZ^*$  ( $ZH_3^{0*}$ ),  $W^+W^{*-}$  ( $W^+H_3^{-*}$ ), and charge conjugate, and the  $H_3f\bar{f}$  channels  $H_3^0Z^*$  ( $H_3^0H_3^{0*}$ ), and  $H_3^+W^{*-}$  ( $H_3^+H_3^{-*}$ ), and charge conjugate. In the  $BB$  region we must consider  $VV$  channels  $ZZ$  and  $W^+W^-$ ;  $H_3V$  channels  $H_3^0Z$ ,  $H_3^+W^-$ , and  $H_3^-W^+$ ; and  $H_3H_3$  channels  $H_3^0H_3^0$  and  $H_3^+H_3^-$ . Finally, as in the case of the  $H_5^+$ , we must include the  $f\bar{f}$  decay modes induced at one-loop, e.g., via the finite triangle-type diagrams. These will be dominant for  $m_{H_5}$  below and somewhat into the  $BB^*$  region. Thus, the  $H_5^0$  becomes invisible only when it is extremely light (roughly for  $m_{H_5} < 2m_\mu$ ). At higher mass, decay patterns in the  $BB^*$  and  $BB$  regions are extremely similar to those already presented for the  $H_5^{++}$  and  $H_5^+$  and will not be given here. While the  $H_5^0$  is not as easily searched for at current machines as its charged partners, in the present model, where all the  $H_5$ 's are degenerate, we will soon know that it cannot be lighter than  $\sim m_Z/2$ .

The final Higgs boson to consider is the  $H_1^{0'}$ . As already remarked, when  $\lambda_3 = 0$  and the  $H_1^0$  and  $H_1^{0'}$  do not mix, the  $H_1^{0'}$  has no tree-level  $f\bar{f}$  couplings. However, it is likely that  $\lambda_3$  is not exactly zero. Then, at low mass (in the  $B^*B^*$  region) the decays of the  $H_1^{0'}$  will be dominated by the mixing-induced  $f\bar{f}$  channels. (Recall that even if  $\lambda_3 = 0$ , one-loop triangle-diagram-induced  $f\bar{f}$  couplings will dominate this region.) However, as  $m_{H_1^{0'}}$  increases and we move into the  $BB^*$  region and then the  $BB$  decay region, these mixing-induced  $f\bar{f}$  decays will become unimportant. (The exact crossover point is clearly determined by the precise value of  $\lambda_3$ .) There are then many channels to consider. In the  $BB^*$  region we have  $Vf\bar{f}$

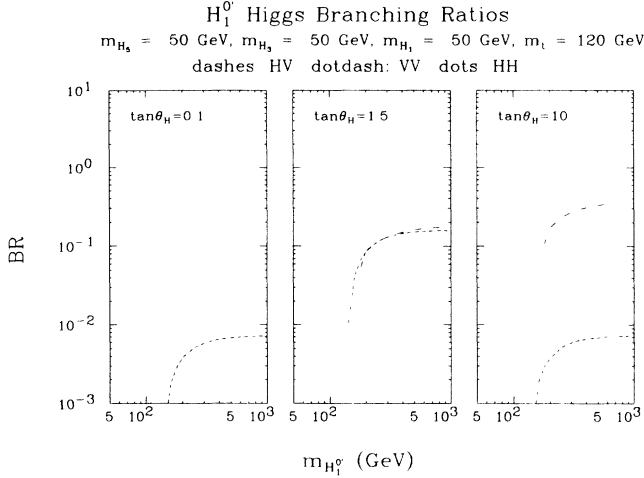


FIG. 8.  $VV$ ,  $HV$ , and  $HH$  branching ratios for the  $H_1^0$  in the limit of  $\lambda_3=0$  (for which  $H_1^0$  does not decay to  $f\bar{f}$ ). See text for more details.

channels  $W^+W^{*-}$  ( $W^+H_3^{*-}$ ), the charge conjugate, and  $ZZ^*$  ( $ZH_3^{0*}$ );  $Hf\bar{f}$  channels  $H_3^+W^{*-}$  ( $H_3^+H_3^{*-}$ ), its charge conjugate, and  $H_3^0Z^*$  ( $H_3^0H_3^{0*}$ ). In the  $BB$  region we have  $VV$  channels  $W^+W^-$  and  $ZZ$ ;  $HV$  channels  $H_3^+W^-$ ,  $H_3^-W^+$ , and  $H_3^0Z$ ; and  $HH$  channels  $H_3^+H_3^-$ ,  $H_3^0H_3^0$ ,  $H_5^+H_5^-$ ,  $H_5^+H_5^0$ , and  $H_5^0H_5^0$ .<sup>19</sup> In Fig. 8 we illustrate the  $BB$  branching ratios for the  $H_1^0$ , taking  $m_{H_3}=m_{H_4}=m_{H_5}=50 \text{ GeV}$ . The interesting feature is the complete dominance of the Higgs pair modes. In fact, it is the  $H_5H_5$  modes which are the largest; at  $\tan\theta_H=0.1$ , the  $H_3H_3$  modes are only slightly smaller, but by  $\tan\theta_H=10$ , the  $H_3H_3$  modes are very much smaller. This occurs because (in the mass range considered)  $\lambda_2$  is the largest term in the  $H_1^0H_3H_3$  and  $H_1^0H_5H_5$  couplings of Eq. (2.22). Thus, at large  $\tan\theta_H$  where  $c_H$  is small, the former couplings are suppressed since  $\lambda_2$  is multiplied by  $c_H^2$ . This also has the implication that if the  $H_5H_5$  channels are not allowed, then the  $H_3H_3$  channels are only dominant at small  $\tan\theta_H$ ; at large  $\tan\theta_H$  the  $VV$  channels will be dominant when  $H_5H_5$  channels are kinematically forbidden. But, if the  $H_5H_5$  channels are allowed, we see that the  $H_1^0$  is likely to decay to final states of great complexity; if  $m_{H_5}$  is such that the  $H_5$ 's are all decaying in the  $BB^*$  or  $BB$  regions, each  $H_5$  final state will contain two fermion-antifermion pairs, and the  $H_1^0$  will have four fermion-antifermion pairs as its signature.

Thus, we see that there is tremendous diversity in the decay modes of Higgs bosons of the model. We now turn to a discussion of the production mechanisms for the Higgs bosons, and prospects for their detection given the decays just discussed.

## VI. PRODUCTION MECHANISMS AND DETECTION

Let us now briefly survey the production and detection phenomenology of the  $H_5$ ,  $H_3$ ,  $H_1^0$ , and  $H_1^{\pm}$  Higgs bosons

in light of their couplings and decays. This survey will presume some rough familiarity with the related phenomenology for other nonminimal Higgs models, such as the two-doublet extension of the SM and the minimal supersymmetric model. It is meant only to provide a crude guide and is by no means complete.

### A. Low-energy experiments

If any of the neutral or charged Higgs bosons of the model have very low masses, then low-energy experiments may be sensitive to them. For instance, rare  $\pi$ ,  $K$ ,  $B$ , and  $\Upsilon$  decays should be considered. As an example,  $\Upsilon$  decays would be an excellent place to search for  $H_3^0$  and  $H_1^0$ ,<sup>20</sup> but would not be useful in searching for a very light  $H_5^0$  or  $H_1^{\pm}$  (which have no tree-level  $f\bar{f}$  couplings). In the case of the SM  $\phi^0$ ,  $\Upsilon$  decay results are not conclusive.<sup>1</sup> However, if the  $b\bar{b}$  coupling of the  $H_3^0$  or  $H_1^0$  is enhanced by 50% or more compared to the SM value, then  $\Upsilon$  decays eliminate Higgs-boson masses in the range 600 MeV to  $\sim 5 \text{ GeV}$ . Limitations on the  $H_3^0$  and  $H_1^0$  from rare  $\pi$ ,  $K$ , and  $B$  decays require more careful assessment and will not be pursued here. Turning to the charged Higgs bosons of the model, we have already seen that  $B$ - $\bar{B}$  mixing would be very sensitive to the  $H_3^+$ , but not to the  $H_5^+$ . And, of course, low-energy experiments are not sensitive to the  $H_5^{++}$ , since it has no fermion-antifermion couplings.

### B. Z factories

Moving to slightly higher Higgs-boson masses, we note that Eq. (2.15) makes it clear that on-shell  $Z$  decays would be a copious source of Higgs pairs of all kinds. The branching ratio for the decay  $Z \rightarrow h_1 h_2$  (where  $h_1$  and  $h_2$  are any two Higgs bosons) is given as

$$\frac{\Gamma(Z \rightarrow h_1 h_2)}{\Gamma(Z \rightarrow \nu\bar{\nu})} = \frac{1}{2} f^2 B^3, \quad (6.1)$$

where  $B \equiv 2|\mathbf{p}|/m_Z$  ( $|\mathbf{p}|$  is the magnitude of the three-momentum of one of the Higgs bosons in the  $Z$  rest frame). In Eq. (6.1) the quantity  $f$  specifies the strength of the  $Zh_1 h_2$  coupling with Feynman rule given by the generic form

$$Zh_1 h_2: \frac{igf}{2 \cos\theta_W} (p_1 - p_2) \cdot \epsilon_Z, \quad (6.2)$$

where  $p_1$  and  $p_2$  are the (incoming) momenta of  $h_1$  and  $h_2$ , respectively. Thus, the relevant quantities  $f$  for each possible Higgs pair are exactly the coefficients listed in the middle column of Eq. (2.15). Note, in particular, that for neutral Higgs pairs one is always the  $H_3^0$  while the other is an  $H_i^0$ , where  $H_i^0 = H_5^0$ ,  $H_1^0$ , or  $H_1^{\pm}$ . For these cases, it will be convenient to introduce the notation  $f \equiv f_{H_i^0}$  for the coupling strength factor.

Barring extreme values for  $\tan\theta_H$ , the coupling strengths  $f$  are such that if all the Higgs bosons of this model have mass less than  $\sim m_Z/2$ , then all could be discovered with about  $10^4$   $Z$  decays. In the case of  $Z \rightarrow H_5^{++} H_5^{--}$ , for instance, we find  $f^2 = 4 \cos^2 2\theta_W$ ,

yielding a very large rate according to Eq. (6.1). Of course, the experimental search for such decays must account for the fact that the  $H_5^{++}$  and  $H_5^{--}$  would decay to two  $f\bar{f}'$  pairs each. Other  $Z$  to Higgs pair decay channels do not have such a large rate, but the final state would be more conventional. Indeed, in the mass range below  $\sim m_Z/2$ , we have seen that it is most probable that all the singly charged and neutral Higgs bosons would decay to fermion-antifermion pairs, either by tree-level couplings (in the case of  $H_3$ 's) or by one-loop and/or mixing-induced couplings (in the case of  $H_5^+$ ,  $H_5^0$ , and  $H_1^0$ ). An exception to the latter occurs if one of the Higgs bosons is so light that  $HH$  modes become important in the decay of one of the produced primary Higgs bosons. A particularly exotic example of such a situation arises if  $2m_{H_5} < m_{H_1^0}$ . For moderate  $\tan\theta_H$ , the  $f$  value obtained from Eq. (2.15) implies a reasonable rate for  $Z \rightarrow H_3^0 H_1^0$ , Eq. (2.19) implies that  $m_{H_1^0}$  need not be small, and Eq. (2.22) implies significant  $H_1^0 \rightarrow H_5^+ H_5^0, H_5^+ H_5^-, H_5^+ H_5^{--}$  branching ratios if kinematically allowed. (Of course, if  $m_{H_5}$  is small enough for this to happen, the decays  $Z \rightarrow H_5^+ H_5^-, H_5^{++} H_5^{--}$  would be very obvious.) Another example is the decay  $Z \rightarrow H_5^0 H_3^0$  followed by  $H_5^0 \rightarrow H_3^+ H_3^0, H_3^+ H_3^-$  if  $2m_{H_3} < m_{H_5}$ .

Continuing on to other production modes, from Eq. (2.14), we see that  $Z \rightarrow l^+ l^- H_i^0$ , the rate for which is controlled by the  $ZZH_i^0$  coupling strength, is possibly useful for  $H_i^0 = H_5^0, H_1^0$ , and  $H_1^0$ , but not for  $H_i^0 = H_3^0$ . Thus, even if  $m_{H_3}$  is larger than  $m_Z$  (as suggested, but not required, by  $B\text{-}\bar{B}$  mixing) and one cannot use the pair-production discovery mode, all the neutral Higgs bosons except the  $H_3^0$  could be searched for up to about 40 GeV in mass, using  $10^5$  to  $10^7$   $Z$  decays (depending upon  $\tan\theta_H$ ). On the other hand, searches for a neutral Higgs boson in  $\Theta \rightarrow \gamma H_i^0$  would only be possible for  $H_i^0 = H_3^0$  and  $H_1^0$ .

### C. High-energy hadron colliders

At still higher masses, we must consider possibilities for detection of the various Higgs bosons of this model at high-energy colliders. Let us first focus on hadron colliders. We shall discuss results for the Superconducting Super Collider (SSC), but analogous considerations would also apply at the CERN Large Hadron Collider (LHC). We remind the reader that there are a number of basic production mechanisms of possible relevance:<sup>1</sup> gluon-gluon fusion for neutral Higgs bosons with  $q\bar{q}$  couplings;  $VV$  fusion for any Higgs boson (neutral or charged) with tree-level  $VV$  couplings; and either  $t \rightarrow H^+ b$  (for  $m_t > m_H + m_b$ ) or  $g\bar{b} \rightarrow H^+ \bar{t}$  for any charged Higgs boson with quark couplings. We discuss each in turn.

In gluon-gluon fusion a neutral Higgs boson is produced via  $ggH_i^0$  couplings arising from one-loop graphs in which the  $H_i^0$  couples to quarks. From Eq. (2.13) we have already learned that only  $H_1^0$  and  $H_3^0$  have tree-level  $q\bar{q}$  couplings. From this equation we see that  $gg$  fusion to  $H_1^0$  is simply obtained from results for the SM Higgs boson ( $\phi^0$ ) by multiplying by  $c_H^{-2}$ .  $B\text{-}\bar{B}$  mixing suggests that

$c_H$  cannot be too small, implying that  $H_1^0$  production via gluon fusion will be somewhat, but not enormously, enhanced compared to results for the  $\phi^0$ . For the  $H_3^0$ , we must be more careful because of the alternating sign of the coupling [appearing in Eq. (2.13)] to up- and down-type quarks. In addition, the  $H_3^0$  and  $\gamma_5$  coupling to quarks. For this (pseudoscalar) coupling, a single heavy quark loop contributes  $\frac{3}{2}$  times the result for scalar coupling. Of course, the most important unknown in computing  $gg$  fusion processes is the mass of the top quark. The cross sections for  $H_1^0$  and  $H_3^0$  production at the SSC are illustrated in Fig. 9, for the case of  $m_t = 120$  GeV. No rapidity cuts have been incorporated. However, we have imposed the requirement  $x \geq 10^{-4}$  on the  $x$  values at which the gluon distribution functions are evaluated. We have also taken the  $Q$  value at which these distributions are evaluated to be  $Q = m_{\text{Higgs}}$ . These cross sections have been computed in the simplest approximation, where the Higgs boson is treated as an on-shell particle. Once the Higgs-boson mass is  $\gtrsim 1$  TeV, the reliability of the on-shell approximation becomes uncertain. However, even a full perturbative calculation of the  $gg$  fusion production of  $VV$  pairs would not necessarily give a more accurate result since the interactions in the  $VV$  channel become strong at high  $m_{\text{Higgs}}$ . Nonetheless, it is clear that this mechanism yields substantial cross sections out to large masses.

The next mechanism of interest is the  $VV$  fusion process. The relevant couplings appear in Eq. (2.14). Clearly, all Higgs bosons other than the  $H_3^+$  and  $H_3^0$  can be produced in this way. We have computed the cross sections at the SSC and our results are presented in Fig. 10. As for the  $gg$  fusion computation, we have required  $x \geq 10^{-4}$  for the parton distribution function variables, and have taken  $Q = m_{\text{Higgs}}$ . The same on-shell approximation is used, and the same cautionary remarks apply for  $m_{\text{Higgs}} \gtrsim 1$  TeV. Clearly, the cross sections are gen-

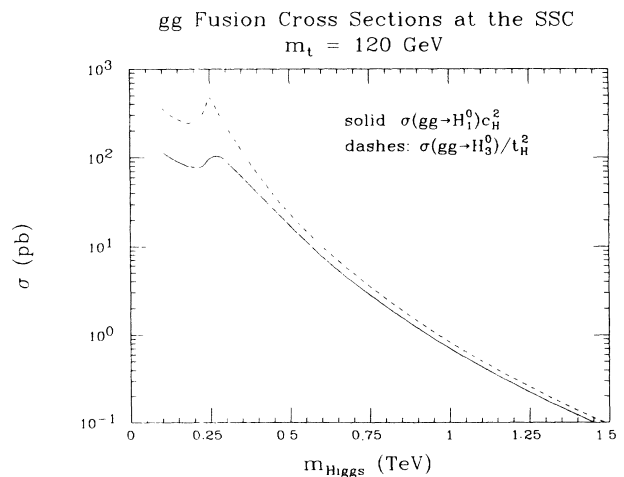


FIG. 9. Cross sections from  $gg$  fusion for  $H_1^0$  (solid line) and  $H_3^0$  (dashed line). A factor of  $c_H^{-2}$  has been removed from the  $H_1^0$  cross section, and a factor of  $t_H^2$  from the  $H_3^0$  cross section. We have taken  $m_t = 120$  GeV. The solid curve also gives the cross section for the SM  $\phi^0$ .

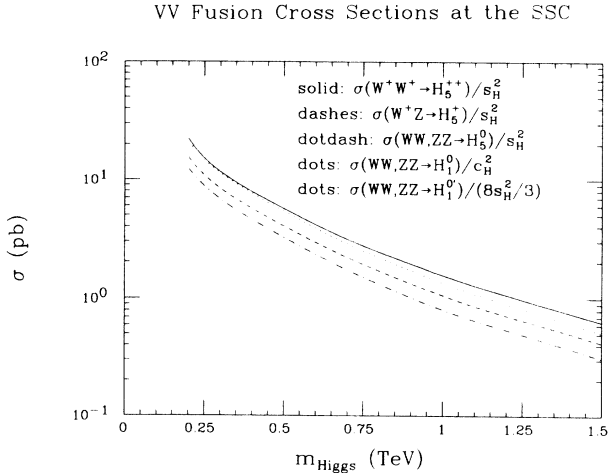


FIG. 10.  $VV$  fusion cross sections for  $H_1^0$ ,  $H_1^{0'}$ ,  $H_3^0$ ,  $H_5^+$ , and  $H_5^{++}$  as a function of Higgs-boson mass at the SSC. The legend indicates the factors involving  $s_H$  or  $c_H$  that have been removed in presenting the results. Note that the dotted curve is also the prediction for the SM  $\phi^0$ .

erally somewhat suppressed compared to those predicted for the SM  $\phi^0$  by the factors depending upon  $s_H$  or  $c_H$ . However, for moderate  $\tan\theta_H$  this suppression would be a factor of only 2 or 3, and one in general obtains cross sections of order 1 pb at Higgs-boson masses near 1 TeV. Comparing to Fig. 9, we see that for  $m_t = 120$  GeV the  $VV$  fusion cross sections are typically somewhat larger than the  $gg$  fusion cross sections only for  $m_{\text{Higgs}} \gtrsim 0.8$  TeV, depending, of course, on the factors involving  $s_H$ ,  $c_H$ , and  $t_H$ .

The case of the doubly charged Higgs boson has been explored in greater depth in Ref. 21. They have examined the influence of the full Higgs sector of this model (in particular, of  $W^+W^+ \rightarrow H_5^{++}$  followed by  $H_5^{++} \rightarrow W^+W^+$  decay to real  $W$ 's) upon the  $W^+W^+ \rightarrow W^+W^+$  scattering process. For moderate values of the  $H_5^{++}$  mass, in the range 0.5 to 1 TeV, they find a large peak in the  $W^+W^+$  mass spectrum, the height of which is roughly  $\tan\theta_H$  independent. (In the approximation used in Ref. 21, the  $HV$  and  $HH$  decay modes are neglected. Then, even though the integrated cross section is smaller for small  $\tan\theta_H$ , the width of the  $H_5^{++}$  also decreases as  $\tan\theta_H$  decreases, so that the peak cross section remains approximately constant.) The extent to which one can make use of the large peak resulting from a narrow width is not clear. If both  $W^+$ 's are detected in their leptonic mode, then the missing neutrinos will greatly broaden the peak. A final state in which one  $W^+$  decays leptonically and the other  $W^+$  hadronically may give better resolution, but it may still not be adequate to make use of the narrow peak; a detailed study is required. Certainly, for  $\tan\theta_H \lesssim 1$  it begins to become doubtful that the presence of the  $H_5^{++}$  would be detectable above the  $qq \rightarrow qqW^+W^+$  background at the SSC.

Indeed, if  $s_H$  is small then the  $W^+W^+$  fusion cross section is not large, and, if, in addition,  $H_3^+H_3^+$  decays are

kinematically allowed, Fig. 5 shows that the  $W^+W^+$  decay mode of the  $H_5^{++}$  will no longer be dominant. Consideration must be given to the observability of the  $H_3^+H_3^+$  decay channel of the  $H_5^{++}$ . This latter depends on many details. For instance, if  $f\bar{f}'$  modes dominate  $H_3^+$  decay (see Fig. 1), the dominant  $H_3^+$  decay is likely to be  $H_3^+ \rightarrow t\bar{b}$  when all the Higgs bosons are reasonably heavy. Whether or not  $t \rightarrow W^+b$  is a real or virtual decay, the background in this channel from  $t\bar{t}$  production followed by  $t$  decay is likely to be a problem. On the other hand, if the  $H_3^+$  is fairly light,  $H_3^+ \rightarrow \tau^+\nu$  would be an important channel and might stand out from backgrounds. Of course, if  $H_1^0W^+$  or  $H_1^{0'}W^+$  channels dominate  $H_3^+$  decays (as occurs when  $\tan\theta_H$  is small and  $H_5$  channels are kinematically forbidden—the latter being implicit in the present situation)  $H_5^{++}$  decay final states containing an  $H_3^+$  would have rather complicated signatures. Clearly, detailed studies of the background and signal characteristics and cross sections are required. These are beyond the scope of the present work. However, they are typical of the type of work that is needed in order to fully assess the observability of the Higgs bosons of this model when produced via  $VV$  and/or  $gg$  fusion at the SSC.

For singly charged Higgs bosons with  $f\bar{f}'$  tree-level couplings, namely, the  $H_3^+$  in the present model, the primary production mechanisms to consider are two. If  $m_t > m_{H_3^+} + m_b$ , then  $t\bar{t}$  production followed by  $t \rightarrow H_3^+b$  and  $\bar{t} \rightarrow H_3^- \bar{b}$  could provide a copious source of charged  $H_3$ 's. This  $t$  decay mode would dominate  $t \rightarrow W^+b$  (if allowed) when  $\tan\theta_W$  is big. The  $H_3^+$  would then decay (most probably  $HV$  modes are all kinematically forbidden in this scenario) to  $\tau^+\nu$  and  $c\bar{s}$ . Techniques for isolating the  $\tau^+\nu$  signal have been developed and are reviewed in Ref. 1. If the  $H_3^+$  is too heavy to appear in  $t$  decays, then the only production mode with possibly usable cross section is  $g\bar{b} \rightarrow H_3^+ \bar{t}$  (and its charge conjugate). The cross section from this source, and the very severe backgrounds arising from  $g\bar{b} \rightarrow W^+ \bar{t}$  (and its charge conjugate) are also reviewed in Ref. 1. These background studies assume dominance of  $f\bar{f}'$  decay modes for the  $H_3^+$ . Only if this production cross section happens to be greatly enhanced by a large value for  $\tan\theta_H$  (not likely given  $B-\bar{B}$  mixing constraints unless  $m_{H_3^+}$  is quite large) is detection conceivable. Of course, if  $\tan\theta_H$  is smaller, and  $HV$  channels are kinematically allowed for the  $H_3^+$  decays (see Fig. 1 and associated discussion), even though the cross section would be relatively smaller, the signature might be much more distinct. An entirely different background study must be performed.

#### D. High-energy $e^+e^-$ colliders

Let us now turn to  $e^+e^-$  colliders. Consider first the doubly charged Higgs boson. At an  $e^+e^-$  collider,  $W^+W^+$  fusion is not possible and one would turn to  $H_5^{++}H_5^{-}$  pair production via virtual  $Z^*$  and  $\gamma^*$  exchange. The cross section for pair production is easily obtained from our Feynman rules of Eq. (2.15). Using the notation  $s_W \equiv \sin\theta_W$  and  $c_W \equiv \cos\theta_W$ , we find

$$\sigma(H_5^+H_5^{--}) = \frac{g^4\beta^3}{48\pi s} \left[ (2s_W^2)^2 + \frac{1}{2} \frac{(1-2s_W^2)^2}{c_W^4} \left( \frac{s}{s-m_Z^2} \right)^2 (a_L^2 + a_R^2) - \frac{2s_W^2(1-2s_W^2)}{c_W^2} \frac{s}{s-m_Z^2} (a_L + a_R) \right], \quad (6.3)$$

where  $\sqrt{s}$  is the  $e^+e^-$  center-of-mass energy,  $\beta = \sqrt{1-4m_{H_5}^2/s}$ , and  $a_L = -\frac{1}{2} + s_W^2$  and  $a_R = s_W^2$  are the left- and right-handed couplings of the  $Z$  to  $e^+e^-$ . At very large  $s$  it is convenient to express this result in units of  $R$ , where  $R \equiv \sigma/\sigma_{\text{pt}}$  and

$$\sigma_{\text{pt}} \equiv \sigma(e^+e^- \rightarrow \mu^+\mu^-) = \frac{4}{3}\pi\alpha^2/s.$$

We find

$$R_{H_5^+H_5^{--}} \rightarrow \frac{1+4\sin^4\theta_W}{2\sin^4 2\theta_W} \simeq 1.2, \quad (6.4)$$

where we have employed  $\sin^2\theta_W = 0.23$ . (Amusingly,  $2\sin^4 2\theta_W \simeq 1$  for  $\sin^2\theta_W \simeq 0.23$ , and we see immediately that the result is slightly above 1 unit of  $R$ .) Including the phase-space factor, we obtain the cross section in units of  $R$  illustrated in Fig. 11. Clearly, when phase-space suppression is not large, the cross section is substantial. Detection of the  $H_5^{++}$  and  $H_5^{--}$  must take into account the different possible decay scenarios discussed in connection with Figs. 4 and 5. The  $H_5^{++}$  decays would, in general, yield a mixture of  $W^+W^+$ ,  $H_3^+W^+$ , and  $H_3^+H_3^+$  states. Or, if the real channels are not allowed, such channels as  $W^+l^+\nu$  when one real  $W$  is possible, or when the  $H_5^{++}$  mass is below  $m_W$ ,  $l^+\nu l^+\nu$  channels become important. In fact, as already mentioned, at low  $m_{H_5}$  the  $H_5^{++}$  will not decay in the detector. At high  $m_{H_5}$ ,  $H_3^+H_3^+$  (if allowed) will dominate if  $\tan\theta_H$  is small; then, if the  $H_3^+$  decays to  $ff'$  channels, the  $H_5^{++}H_5^{--}$  pair must be examined in an eight-fermion

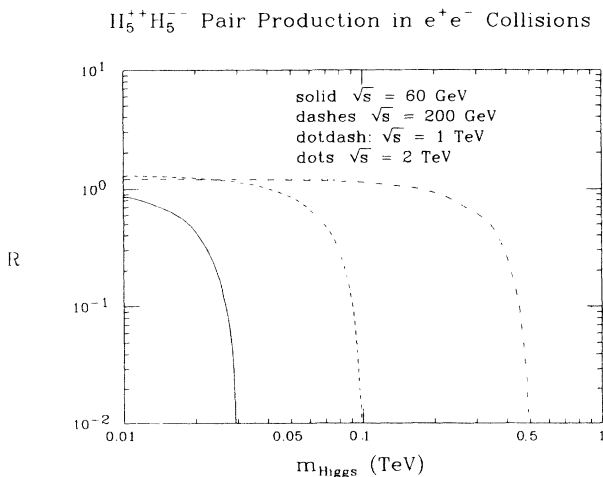


FIG. 11. Cross section for  $e^+e^- \rightarrow H_5^{++}H_5^{--}$  (in units of  $R$ ) as a function of  $m_{H_5} = m_{\text{Higgs}}$ , for the indicated  $\sqrt{s}$  values. Cross sections for  $e^+e^- \rightarrow H_5^+H_5^-$  and  $e^+e^- \rightarrow H_3^+H_3^+$  are obtained by dividing by a factor of 4, and identifying  $m_{\text{Higgs}}$  with  $m_{H_5}$  or  $m_{H_3}$ , respectively.

final state—the heaviest fermion channels being preferred.

There could also be substantially new phenomenology for the singly charged Higgs sector. In  $e^+e^-$  collisions, if  $s_H$  is not too small, the singly charged  $H_5^+$  could be made with substantial rate by the associated production process,  $e^+e^- \rightarrow Z^* \rightarrow W^-H_5^+$ , or at higher  $\sqrt{s}$  by the  $W^+Z$  fusion process,  $e^+e^- \rightarrow e^+e^-W^+Z^* \rightarrow e^+e^-H_5^+$ . These cross sections are plotted in Fig. 12; they should be doubled to include the  $H_5^-$  production rate. Because of the relatively weak coupling of the  $Z$  to the electron, the associated production process is dominant over the fusion process out to larger  $\sqrt{s}$  values than in the standard-model Higgs case to be reviewed shortly. Nonetheless, the  $W^+Z$  fusion reaction quickly becomes dominant as  $\sqrt{s}$  increases at fixed Higgs-boson mass. However, if  $s_H$  is small, these  $W^-ZH_5^+$ -coupling-mediated processes are suppressed by a factor of  $s_H^2$ , and the  $\gamma^*, Z^* \rightarrow H_5^+H_5^-$  pair-production process could become the most (when phase space is allowed). As mentioned in the caption to Fig. 11, the cross section for  $H_5^+H_5^-$  pair production is simply obtained by taking  $\frac{1}{4}$  of the  $H_5^{++}H_5^{--}$  pair cross section. Regarding the  $H_5^+$  signal, we refer to the discussion of decays in connection with Fig. 7. At high mass the  $H_5^+$  tree-level decays are into  $W^+Z$ ,  $H_3^0W^+$ ,  $H_3^+Z$ , and  $H_3^+H_i^0$ , where  $H_i^0 = H_3^0$ ,  $H_1^0$  or  $H_1^0$ . Particularly interesting is the  $W^+Z$  channel.

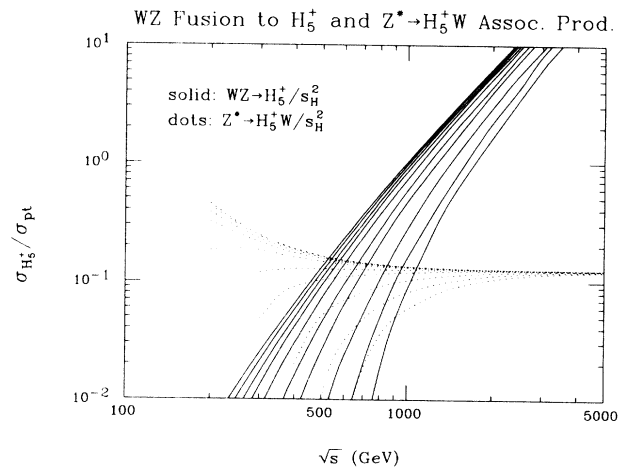


FIG. 12. Cross sections for  $H_5^+$  production in  $e^+e^-$  collisions deriving from  $W^+Z$  fusion (solid line) and  $Z^* \rightarrow H_5^+W^-$  (dashed line). We normalize relative to the point cross section for  $e^+e^- \rightarrow \mu^+\mu^-$ ,  $\sigma_{\text{pt}}$ . The different lines of a given type correspond to  $m_{H_5}$  values of 10, 30, 50, 70, 100, 150, 200, 300, 400, and 500 GeV. Cross-section curves always decrease in magnitude with increasing  $m_{H_5}$ . The results graphed are to be multiplied by  $s_H^2$ .



As already emphasized, this channel of decay is not possible for the singly charged Higgs bosons found in models not containing Higgs-triplet fields, and will dominate  $H_5^+$  decays (when allowed) at moderate to large  $\tan\theta_H$  where the associated production and fusion cross sections are also substantial.

In contrast to the  $H_5^-$ , the  $H_3^+$  has no tree-level  $W^+Z$  coupling; instead, as we have noted, its fermion couplings could be greatly enhanced if  $\tan\theta_H \gg 1$ . Thus, at an  $e^+e^-$  collider, in addition to the pair-creation process, bremsstrahlung from a heavy top quark could also become an important source of  $H_3^+$  production. Further, if the  $H_3^+$  is light enough to appear in  $t \rightarrow H_3^+ b$  decays and if it has enhanced fermion couplings, then such decays would totally dominate over the SM  $t \rightarrow W^+ b$  decays. Of course, a light  $H_3^+$  in combination with large  $\tan\theta_H$  may turn out to be inconsistent with weak-interaction and/or  $B-\bar{B}$  mixing constraints, as we have discussed. But, should the  $t \rightarrow H_3^+ b$  branching ratio be significant, the  $H_3^+$  might not decay conventionally. In particular, since  $H_3^+ \rightarrow t\bar{b}$  is not allowed in this scenario, the decays of the  $H_3^+$  might not be totally dominated by fermion channels. We have emphasized in connection with Fig. 1 that, depending upon the size of  $\tan\theta_H$ , channels with Higgs pairs or a Higgs boson plus a vector boson could become important; but the  $W^+Z$  channel would not be present.

Turning to the neutral Higgs states, we note from Eq. (2.14) that  $H_5^0$ ,  $H_1^0$ , and  $H_1^0$  all have  $H^0W^+W^-$  and  $H^0ZZ$  couplings, and can be produced at an  $e^+e^-$  collider using the vector-boson fusion and associated production processes. In the case of  $H_5^0$  and  $H_1^0$ , as long as  $s_H$  is not small the cross sections for these two reactions can be substantial. The  $H_1^0$  cross section is large when  $c_H$  is substantial. From Eq. (2.14), we see that the  $W^+W^-$  fusion cross sections for these three Higgs bosons are easily obtained relative to that for the SM  $\phi^0$  by the ratios

$$H_5^0:H_1^0:H_1^0:\phi^0 = \frac{1}{3}s_H^2:\frac{8}{3}s_H^2:c_H^2:1. \quad (6.5)$$

(We neglect  $ZZ$  fusion since it is much smaller than  $W^+W^-$  fusion due to the small  $Ze^+e^-$  coupling strength.) In the case of the associated production mechanism the cross-section ratios are

$$H_5^0:H_1^0:H_1^0:\phi^0 = \frac{4}{3}s_H^2:\frac{8}{3}s_H^2:c_H^2:1. \quad (6.6)$$

As a reference, we give the cross sections for  $W^+W^- \rightarrow H^0$  fusion and  $Z^* \rightarrow H^0Z$  associated production, computed for SM  $\phi^0$  couplings, in Fig. 13. In assessing the detectability of an  $H^0$  produced alone, or in association with a  $Z$ , it will, of course, be important to take into consideration its decays. As noted earlier,  $H_5^0$  has decay patterns very similar to its charged counterparts. When  $\tan\theta_H$  is large and associated production and fusion cross sections are substantial, it will decay mainly to the  $W^+W^-$  and  $ZZ$  final states (if kinematically allowed). In contrast, the decays of both the  $H_1^0$  and  $H_1^0$  can be dominated by Higgs-pair final states, see Figs. 3 and 8 and associated discussion. In particular,  $H_5H_5$  pairs can be important if kinematically allowed; the subsequent  $H_5$  decays can lead to final-state signatures re-

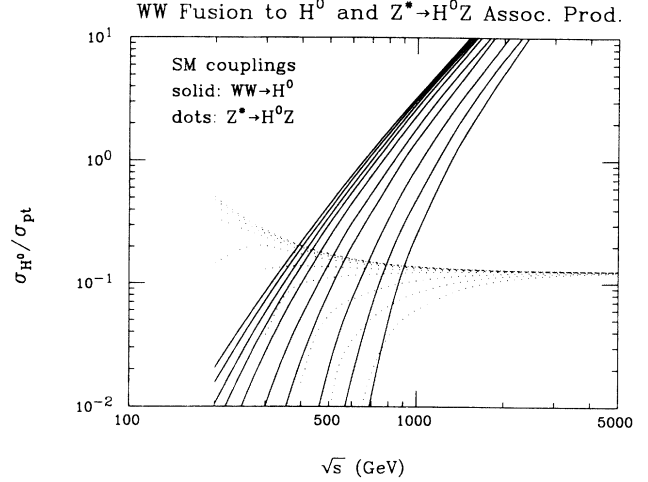


FIG. 13. Cross sections for  $H^0$  production in  $e^+e^-$  collisions deriving from  $W^+W^-$  fusion (solid line) and  $Z^* \rightarrow H^0Z$  (dashed line). We normalize relative to the point cross section for  $e^+e^- \rightarrow \mu^+\mu^-$ ,  $\sigma_{pt}$ . The different lines of a given type correspond to  $m_{H^0}$  values of 10, 30, 50, 70, 100, 150, 200, 300, 400, and 500 GeV. Cross-section curves always decrease in magnitude with increasing  $m_{H^0}$ . The cross sections given are those for SM couplings. Results for the  $H_5^0$ ,  $H_1^0$ , and  $H_1^0$  are obtained using the ratios quoted in the text.

quiring sensitivity to eight fermions.

The  $H_3^0$ , a pseudoscalar with no  $VV$  couplings but (possibly enhanced) fermion couplings, would be produced at an  $e^+e^-$  collider in association with neutral-scalar Higgs bosons via the mechanism  $e^+e^- \rightarrow Z^* \rightarrow H_3^0H_i^0$  with  $H_i^0 = H_1^0$ ,  $H_1^0$ , or  $H_5^0$ ; the cross section for the  $H_3^0$  is large when  $s_H$  is not small, while the latter two modes have large cross sections when  $c_H$  is substantial. Using the couplings of Eq. (2.15) and the definition of  $f_{H_i^0}$  following Eq. (6.2), the cross section for  $H_3^0H_i^0$  may be written in the form

$$\sigma(Z^* \rightarrow H_3^0H_i^0) = \frac{g^4 f_{H_i^0}^2}{48\pi} \frac{a_L^2 + a_R^2}{\cos^4\theta_W} \times \frac{\kappa^3}{\sqrt{s} [(s - m_Z^2)^2 + \Gamma_Z^2 m_Z^2]}, \quad (6.7)$$

where  $a_L$  and  $a_R$  are the  $Ze^+e^-$  couplings defined earlier below Eq. (6.3), and  $\kappa = \lambda^{1/2}(s, m_{H_3}^2, m_{H_i^0}^2)/(2\sqrt{s})$ ,  $\lambda(a, b, c) = (a + b - c)^2 - 4ab$ . Clearly, the phase-space suppression depends on both  $m_{H_3}$  and  $m_{H_i^0}$ . However, asymptotically in  $\sqrt{s}$  we obtain the result

$$\frac{\sigma(Z^* \rightarrow H_3^0H_i^0)}{\sigma_{pt}} = f_{H_i^0}^2 \frac{a_L^2 + a_R^2}{2 \sin^4 2\theta_W} \simeq 0.125 f_{H_i^0}^2, \quad (6.8)$$

where we have employed  $\sin^2\theta_W=0.23$ . The decays of the  $H_3^0$  would be to fermions, Higgs pairs, or  $HV$  states. As already discussed, the decays of the  $H_5^0$  would be to  $VV$ -,  $HV$ -, or  $HH$ -type channels, or virtual versions thereof if no real two-body channel is open, or one-loop-mediated  $f\bar{f}$  channels at low  $m_{H_5}$ . In the case of the  $H_1^0$  and  $H_1^{0'}$  one must be especially alert to the possibility of important  $HH$  decay channels at high mass (see Figs. 3 and 8), but at low mass their decays would be dominated by  $f\bar{f}$  channels.

Finally, we wish to point out an important feature of  $e^+e^-$  collisions with regard to production of the neutral Higgs bosons of the model. We have seen that for any  $H_i^0$ , the vector-boson fusion and associated production mechanisms can be suppressed, as can the  $H_3^0H_i^0$  pair-production process. It all depends on  $\tan\theta_H$ . However, there is an important "no-lose" theorem. Examination of the  $W^+W^-H_i^0$  (or  $ZZH_i^0$ ) couplings of Eq. (2.14), and of the  $ZH_3^0H_i^0$  couplings of Eq. (2.15), shows the pattern

$$\begin{aligned} W^+W^-H_5^0 &\propto s_H, & ZH_3^0H_5^0 &\propto c_H, \\ W^+W^-H_1^{0'} &\propto s_H, & ZH_3^0H_1^{0'} &\propto c_H, \\ W^+W^-H_1^0 &\propto c_H, & ZH_3^0H_1^0 &\propto s_H. \end{aligned} \quad (6.9)$$

If  $H_i^0$  production via  $W^+W^-$  fusion (and  $Z^* \rightarrow H_i^0Z$ ) is suppressed, then its production in association with  $H_3^0$  is maximal, and vice versa. Consequently, as long as there is adequate phase space for the Higgs pair-production processes, we will always be able to produce *all* the neutral Higgs bosons of the model at reasonable rates. Of course, it must be admitted that the maximal Higgs pair cross section (slightly more than one-tenth of a unit of  $R$ ) is generally substantially smaller than the maximal vector-boson fusion (though not the associated production) cross section. This fact, coupled with the possibly complex signature for the Higgs pair final state, will obviously make discovery of the Higgs boson(s) that have suppressed  $W^+W^-$  couplings more difficult than discovery of those with substantial  $W^+W^-$  couplings. Nonetheless,  $e^+e^-$  colliders do, in principle, provide an opportunity for discovery of all the neutral (and charged Higgs) bosons of the model, pending a more detailed

study of possible backgrounds to the final states of interest.

## VII. CONCLUSIONS

The Higgs sector extension containing Higgs-triplet representations that we have studied here leads to a considerable complication in Higgs phenomenology. Certainly, the cleanest signature for a Higgs sector with triplet fields would be the discovery of a doubly charged Higgs boson. For moderate to large  $\tan\theta_H$ , relatively clean signatures and copious production mechanisms for the  $H_5^{++}$  of the triplet model we have examined are available at both the SSC and a TeV-scale  $e^+e^-$  collider. If  $\tan\theta_H$  is small, then inclusive production rates for a single  $H_5^{++}$  are suppressed, and one must turn to  $H_5^{++}H_5^{--}$  pair production, having smaller maximal cross section and greater probability of substantial phase-space suppression.

Of course, as  $\tan\theta_H \rightarrow 0$ , the exotic triplet sector of the model has less and less impact on electroweak symmetry breaking, and is less crucial to our unraveling this aspect of the physics. However, a full understanding of the spectrum of spin-0 bosons will be needed to provide important clues and guidance in determining the correct unified gauge theory and associated high-energy symmetries. Here, we have given a first survey of all the relevant phenomenological and theoretical considerations appropriate to the simplest model having Higgs triplets in a custodial SU(2) framework. Our studies indicate that detection of all the Higgs bosons of this model will require examination of a large number of production possibilities and often complicated final states. While further detailed background assessments are clearly needed, it is apparent that both the SSC and a TeV  $e^+e^-$  collider would provide ample opportunities for detection and study of many (and, possibly, all) of the Higgs bosons of the model.

## ACKNOWLEDGMENTS

We would like to thank H. Haber, E. Low, and W. Ko for helpful discussions. This work was supported, in part, by the Department of Energy.

<sup>1</sup>For a review and references, see J. F. Gunion, G. L. Kane, H. E. Haber, and S. Dawson, *The Higgs Hunter's Guide* (Addison-Wesley, Reading, MA, 1989).

<sup>2</sup>For a recent treatment, see J. F. Gunion, J. Grifols, A. Mendez, B. Kayser, and F. Olesch, *Phys. Rev. D* **40**, 1546 (1989).

<sup>3</sup>H. Georgi and M. Machacek, *Nucl. Phys.* **B262**, 463 (1985).

<sup>4</sup>R. S. Chivukula and H. Georgi, *Phys. Lett. B* **182**, 181 (1986).

<sup>5</sup>M. S. Chanowitz and M. Golden, *Phys. Lett.* **165B**, 105 (1985).

<sup>6</sup>See, for example, D. Caldwell, in *Neutrino Masses and Neutrino Astrophysics*, proceedings of the Fourth Telemark Conference, Ashland, Wisconsin, 1987, edited by V. Barger, F. Halzen, M. Marshak, and K. Olive (World Scientific, Singapore, 1987), p. 262.

<sup>7</sup>Particle Data Group, G. P. Yost *et al.*, *Phys. Lett. B* **204**, 1 (1988).

<sup>8</sup>G. B. Gelmini and M. Roncadelli, *Phys. Lett.* **99B**, 411 (1981); H. Georgi, S. L. Glashow, and S. Nussinov, *Nucl. Phys.* **B193**, 297 (1981).

<sup>9</sup>Fermion-antifermion couplings also arise for the  $H_1^{0'}$  at one loop (though not, as mentioned earlier, through mixing with the  $H_3^0$ ,  $Z$ , or  $G_3^0$ ). However, we have already seen that, even at the tree level, there is  $H_1^0$ - $H_1^{0'}$  mixing for  $\lambda_3 \neq 0$ . Thus, when discussing phenomenology for the  $H_1^{0'}$ , we shall presume that it is not an *exact* eigenstate and that it has at least small fermion-antifermion couplings through the  $H_1^0$ . Since these are very likely to be larger than typical of one-loop-induced couplings, we do not discuss one-loop corrections to the  $H_1^{0'}$  couplings to fermion-antifermion channels.

<sup>10</sup>This type of constraint has been studied in the case of the charged Higgs boson of a two-doublet model in J. F. Gunion

and B. Grzadkowski, Report No. UCD-89-30 (unpublished). See also A. J. Buras *et al.*, Report No. MPI-PAE/PTH 52/89 (unpublished); V. Barger, J. L. Hewett, and R. J. N. Phillips, *Phys. Rev. D* **41**, 3421 (1990).

<sup>11</sup>J. F. Gunion and J. Wudka (in preparation).

<sup>12</sup>The more precise versions of this number are reviewed in Ref. 1.

<sup>13</sup>While the complete theory cannot violate unitarity even if  $m_{\phi^0}$  is larger than this value, perturbative calculations are certainly inadequate for higher Higgs-boson masses, since the Higgs sector becomes strongly interacting.

<sup>14</sup>In a multidoublet Higgs model, it is possible for one neutral Higgs boson to be light and also saturate the  $W^+W^-$  and  $ZZ$  couplings. In this case, the other Higgs bosons can all be arbitrarily heavy without encountering unitarity problems.

<sup>15</sup>For  $\lambda_3 \approx 0$ , the value of  $m_{H_1^0}$  enters only in that it determines  $\lambda_2$ .

<sup>16</sup>Since we shall presume that the top quark is heavier than the  $W$ , it could have a big coupling to the  $H_3$ 's and  $H_1^0$ . However, if the  $t\bar{b}$  or  $t\bar{t}$  channels are allowed for the secondary  $H_3^0$  or

$H_1^0$ , the primary  $H_5$  or  $H_1^{0'}$  will be sufficiently massive that three-body modes will already have taken over.

<sup>17</sup>In computing the widths for  $B^*B^*$  or  $BB^*$  modes, all  $f\bar{f}'$  channels coupled to a  $B^*$  are summed over according to the known  $B^*f\bar{f}'$  couplings.

<sup>18</sup>Note that these loop-induced decays can dominate over possible lepton-lepton channels [results for  $c\tau$  in the  $l^+\nu_l$  channel for  $H_5^+$  are rather similar to those for the  $l^+l^+$  channel of  $H_5^{++}$  given in Eq. (5.1)], even if the  $\tau$  family  $h_{\tau\tau}$  saturates its limit, as long as  $s_H^2$  is not small. Any future limits on  $h_{\tau\tau}$  that are stronger by more than a factor of 10 compared to the present limit make it very unlikely that lepton-lepton channels for the  $H_5^+$  (and also the  $H_5^0$  and  $H_1^{0'}$ ) could be of phenomenological relevance.

<sup>19</sup>The  $H_1^0H_1^0$  channel is not accessible in the  $\lambda_3=0$  limit, see Eq. (2.21)

<sup>20</sup>The  $b\bar{b}$  couplings of the latter are always enhanced if  $c_H < 1$ , while those of the former are enhanced if  $\tan\theta_H > 1$ , see Eq. (2.13).

<sup>21</sup>R. Vega and D. A. Dicus, *Nucl. Phys.* **B329**, 533 (1990).